2007

Analysis of Mouse EKLF/KLF2 E9.5 Double Knockout: Yolk Sac Morphology and Embryonic Erythroid Maturation

Tina Kathy Lung
Virginia Commonwealth University

ANALYSIS OF MOUSE EKLF/KLF2 E9.5 DOUBLE KNOCKOUT: YOLK SAC MORPHOLOGY AND EMBRYONIC ERYTHROID MATURATION

A thesis submitted in partial fulfillment of the requirements for the degree of Master of Science at Virginia Commonwealth University.

by

Tina Kathy Lung
Bachelor of Arts, University of Virginia, 2005

Co-director: Dr. Jack Haar
Department of Anatomy and Neurobiology

Co-director: Dr. Joyce Lloyd
Department of Human Genetics

Virginia Commonwealth University
Richmond, Virginia
May 2007

Acknowledgements

First and foremost, I would like to thank my two graduate advisors, Drs. Jack Haar and Joyce Lloyd, both of whom I consulted on a daily basis for advice, guidance, and support. It was a privilege to work with both, where experience and accomplishments in the fields of anatomy and genetics span over 60 years. My sincere appreciation also goes to Dr. Ray Colello, an essential member of my thesis committee, for his patience and advice.

Also, thanks to current graduate students and coworkers, Latasha Redmond, Mohua Basu, Sean Fox, and Megan Smith for their encouragement and technical advice. I am also indebted to Department of Anatomy and Neurobiology's Sue Walker and Judy Williamson, for their help and instruction in histology and microscopy techniques. Julie Farnsworth and Frances White of Flow and Imaging Cytometry Facility also provided generous and invaluable technical support as well as countless cups of tea.

On a personal note, I would like to show appreciation to my friends, all of whom have touched my life in some way. Thanks especially to my two sisters, Connie and Vicki, and brother-in-law, Deo, for their support and encouragement during my years of study. And finally, I owe a special debt of gratitude to my endearing parents, Winston and Kathy, who showed me patience, compassion and encouragement in the face of the demands of graduate study, and whose love fuels my relentless pursuit of research and medicine.

Table of Contents

List of Tables

Page

List of Figures

Page

List of Abbreviations

α	alpha
AGM	Aorta-gonads-mesonephros
AHSP	α-hemoglobin stabilizing protein
β	beta
BFU-E	Burst-forming units-erythroid
cDNA	Complementary DNA
CD71	Transferrin receptor
CFU-E	Colony-forming units-erythroid
chr	chromosome
CLP	Common lymphoid progenitor
CP	Cytoplasmic projection
DNA	Deoxyribonucleic acid
ε	Epsilon
E9.5	Embryonic day 9.5
EKLF	Erythroid Krüppel-like Factor
En	Endothelial cell
Epb4.9	Erythroid protein band 4.9

Epi.....	Epithelial cell
Ery.....	Erythroid cell
EryDs.....	Definitive erythroid cells
EryP-CFC.....	Erythroid progenitor
EryPs.....	Primitive erythroid cells
FITC.....	Fluoroscein
γ.....	gamma
GMP.....	Granulocyte-monocyte progenitor
GPA.....	Glycophorin A
H_20.....	Water
HS.....	DNase I hypersensitive-sites
HSC.....	Hematopoietic stem cell
IGEp.....	Ingrowth of Epithelial Cells
kb.....	kilobase
KLF.....	Krüppel-like Factor
KLF2.....	Krüppel-like Factor 2
KO.....	Knockout
LCR.....	Locus Control Region
LKLF.....	Lung Krüppel-like Factor
M.....	Molar
Mb.....	Megabase
Me.....	Mesothelial cell
MEP.....	Megakaryocyte-erythroid progenitor

MEL.....	mouse erythrolekemia cells
$MgCl_2$.....	magnesium chloride
ml.....	milliliter
mM.....	millimolar
mRNA.....	Messenger RNA
MV.....	Microvilli
NCX1.....	Na+/Ca2+ exchanger
NF-E2.....	Nuclear factor-erythroid 2
PBS.....	phosphate buffered saline
PCR.....	Polymerase Chain Reaction
PE.....	phycoerythrin
RNA.....	ribonucleic acid
rpm.....	revolutions per minute
TAE.....	tris-acetate-EDTA electrophoresis buffer
TfR1.....	Transferrin receptor
Tie2.....	receptor tyrosine kinase Tie2
U.....	unit
µg.....	microgram
µl.....	microliter
VEGFR1.....	Vascular endothelial growth factor (FLK1)
WT.....	Wildtype
YS.....	Yolk sac

Abstract

ANALYSIS OF MOUSE EKLF/KLF2 E9.5 DOUBLE KNOCKOUT: YOLK SAC MORPHOLOGY AND EMBRYONIC ERYTHROID MATURATION

By Tina Kathy Lung, B.A.

A thesis submitted in partial fulfillment of the requirements for the degree of Master of Science at Virginia Commonwealth University.

Virginia Commonwealth University, 2007

Co-Director: Dr. Jack L. Haar
Professor, Department of Anatomy and Neurobiology

Co-Director: Dr. Joyce A. Lloyd
Associate Professor, Department of Human Genetics

Krüppel-like factors (KLFs) are a family of transcription factors with 3 Cys2/His2 zinc fingers that regulate cell differentiation and developmental processes. EKLF is involved in primitive and definitive erythropoiesis; KLF2 is implicated in the development of primitive erythroid and endothelial cells of the vasculature. Using light and electron microscopy, the yolk sacs and dorsal aortae from EKLF/KLF2 double knockout (KO) E9.5 (embryonic day 9.5) were examined to determine whether these KLFs have compensatory functions in morphology of blood cells and vessels. EKLF/KLF2 double KO E9.5 erythroid, endothelial, and mesothelial cells had more

severely abnormal morphology than WT and KLF2-/-. Flow cytometry and cytospins were used to determine maturational effects of single and EKLF/KLF2 double KO primitive erythroid cells double-labeled with anti-TER119 and anti-CD71. EKLF KO and EKLF/KLF2 double KO erythroid cells display defective erythroid maturation. EKLF and KLF2 have overlapping roles in the development of embryonic erythroid and endothelial cells.

CHAPTER I

INTRODUCTION

In this section, the following topics are discussed to familiarize the reader with the background of this study. Beginning with hematopoiesis, there is a review of erythropoiesis and globin gene regulation. With specific focus on the Krüppel-like factors, gene regulation during primitive erythropoiesis and embryo development are examined. Finally, the aims of this study are described.

Hematopoiesis

Vertebrates rely on blood and its properties in order to sustain bodily function and maintenance. The erythroid cell is exclusively designed to optimize the uptake and transport of oxygen and other gaseous molecules to every part of the vertebrate body. The origin of erythroid cells begins with hematopoiesis, which is the development of myeloid and lymphoid cell lineages. The mouse has been extensively studied as a model for human hematopoiesis. Consequently, similarities have been drawn between human and mouse erythroid characteristics resulting in the use of analogous molecular markers for genes as well as invaluable genetic manipulation and application of the mouse model. In the mouse, mesoderm begins to differentiate into angioblastic cords in the extraembryonic yolk sac around embryonic day 7.5 (E7.5). Lying between the visceral endoderm and extraembryonic mesoderm layers of the visceral yolk sac, the cords

develop into blood islands, where centrally located cells become erythroid progenitor cells and peripherally located cells become endothelial cells (Haar, 1971). The visceral yolk sac forms an epithelial cell layer facing the yolk sac cavity and a mesothelial cell layer facing the extraembryonic coelom and embryo. The primitive erythroid cells in the blood islands are the product of primitive erythropoiesis. In addition to primitive erythropoiesis, there is also a definitive hematopoietic lineage from which definitive erythroid cells, megakaryocytes, mast cells, lymphocytes, and other myeloid lineage cells are derived.

Primitive and definitive erythropoiesis in the mouse

Erythropoiesis begins with a primitive (embryonic) population of erythroid cells (EryPs). The cells are characterized by distinct types of progenitors, unique sites of proliferation and maturation, as well as distinguishing size and globin product. In yolk sac blood islands, erythroid progenitors (EryP-CFC) begin to appear at the primitive streak stage, E7.25, and then differentiate into primitive erythroblasts around E7.5 in the mouse yolk sac (Palis, 1999). These progenitors are found in the yolk sac blood islands and can only give rise to the primitive erythroid cell lineage (Wong, 1986). Various erythroblasts or precursors begin circulating in the yolk sac and embryo around E8.25, when mouse cardiac spasm has been reported to trigger the release of EryPs from yolk sac blood islands (Ji, 2003; McGrath, 2003).

While circulating in the blood vessels, precursors differentiate into nucleated large proerythroblasts. These become basophilic proerythroblasts which is the

predominant population from E9.5 to E12.5 (Fraser, 2007), identified mainly by their intense Giemsa stain. From E12.5 to E13.5, orthochromatophilic erythroblasts become the main primitive erythroid precursor circulating in blood. At this time, these cells have lost their nucleoli, while at the same time have started to condense their nuclei and decrease their cell diameter. Orthochromatophilic erythroblasts also stain less intensely with Giemsa due to the loss of basophilic ribosomes (Sasaki, 1985; Fraser, 2007). Eventually, these differentiate into mature reticulocytes, which by E18.5 have become enucleated. It was previously thought that EryPs lost their nuclei between E12.5-E16.5 (Kingsley, 2004), however, Fraser et al (2007) used DNA-binding fluorescent dye DRAQ5 to document exactly when EryPs lost their nuclei over the gestational period of E9.5 to E18.5. They found that fifty percent of circulating EryPs lost their nuclei by E14.5, which gradually increased as the population matured through E18.5. This stable EryP population persists through birth (Kingsley, 2004; Fraser, 2007), but gradually loses the capability to proliferate following approximately 9 days of gestation; at E9.5, EryPs make up 97% of circulating blood (Fraser, 2007).

The onset of primitive erythropoiesis is similar to definitive erythropoiesis. Definitive (adult) erythroid cells (EryDs) develop during a second synchronized wave of erythropoiesis in the mouse and human from a separate population of definitive hematopoietic stem cells (HSCs). Definitive HSCs, present throughout adult life, are self-renewing to support definitive erythropoiesis; this contrasts with EryP-CFC progenitors which remain in the yolk sac only until E9.0 (McGrath, 2005). It was previously reported that yolk sac HSCs most likely did not produce definitive erythroid

cells (Robb, 1997). The intraembryonic AGM (aorta-gonads-mesonephros) region was thought to act as the principle purveyor of definitive HSCs before circulation had fused between yolk sac and embryo at E8.5-9.0 (Cumano, 2000). The AGM is located in the para-aortic splanchnopleura around the embryo dorsal aorta and has been shown to develop after the yolk sac vasculature (Palis, 1995). However, HSCs have been found to originate from both the extraembryonic yolk sac and AGM with subsequent seeding of the fetal liver. Labeled definitive HSCs could be traced from the yolk sac to the fetal liver and adult (Samokhvalov, 2007). Definitive HSCs in the yolk sac are capable of differentiating into definitive fetal liver and bone marrow erythroid precursors; however, definitive HSCs in the AGM only serve to seed the HSCs in the fetal liver. Overall, the fetal liver becomes the predominant site of definitive erythropoiesis by E11.5, which eventually switches to the bone marrow post-natally.

As EryPs start to gradually decrease as a fraction in circulating blood, smaller sized, enucleated EryDs begin a similar differentiation program in the fetal liver around E11.5 (McGrath, 2005). HSCs differentiate into burst-forming units-erythroid (BFU-E) and colony-forming units-erythroid (CFU-E) progenitors. Concurrently, several definitive lineages are derived from the HSCs such as granulocyte-monocyte progenitor (GMP) and megakaryocyte-erythroid progenitor (MEP), and common lymphoid progenitor (CLP) (Ney, 2006). These can go on to form mast cells, megakaryocytes, and lymphocytes around E11.5. Definitive progenitors, BFU-Es and CFU-Es, have been found as early as E8.25 in the yolk sac (Palis, 1999). From these multipotent cells, further differentiation is achieved through the precursor stages of proerythroblast,

basophilic erythroblast, polychromatophilic erythroblast, orthrochromatophilic erythroblast, and reticulocyte. Reticulocytes must lose polyribosomes and nuclei before becoming mature EryDs in the fetal liver. Mature EryDs are three-fold smaller than mature EryPs (Kingsley, 2004). For both primitive and definitive precursors, they lose their nucleoli as proerythroblasts become basophilic erythroblasts; followed by a decrease in cell diameter and cross-section and condensation of nuclei as the cells progress to chromatophilic and orthochromatophilic erythroblasts. Clearly, primitive and definitive erythroid cells undergo similar stepwise maturational stages. This can be conclusively shown with several studies employing flow cytometry to determine erythroid precursor maturation.

Socolovsky et al. (2001) used flow cytometry to isolate definitive erythroid precursors and thus established a maturational profile of these precursors. Using two different markers, erythroid-specific TER119, an unknown protein known to associate with membrane-spanning erythroid protein glycophorin A, and non-erythroid-specific CD71 or transferrin receptor, erythroid cells were simultaneously labeled to determine expression levels. TER119 marker is expressed in early proerythroblasts through mature erythrocytes. Of note, TER119 is not found on cells containing progenitor BFU-E or CFU-E behaviors. CD71 has a 671 amino acid extracellular C-terminal domain in order to bind transferrin, which is required for the binding of iron.

Using this method, erythroid precursors (proerythroblast, basophilic, chromatophilic, and orthochromatophilic erythroblasts) were isolated and characterized with respect to TER119 and CD71 expression in conjunction with cell morphology from

cytospins (Socolovsky, 2001). E14.5 definitive erythroid cells were separated into different maturational stages by regions R1-R5 and confirmed by May Grunwald-Giemsa stain (Figure 1) (Zhang, 2003). Regions are characterized by cell type and TER119 and CD71 expression (Table 1). Hodge et al. (2006) also employed TER119 and CD71 double-labeling in order to look at changes in maturation of EKLF KO E14.5 EryDs and E11.5 EryPs. Fraser et al. (2007) used the method in order to compare maturation profiles specifically of primitive erythroid cells. Although percentages could vary somewhat in R1-R5 regions among mice, they were consistent.

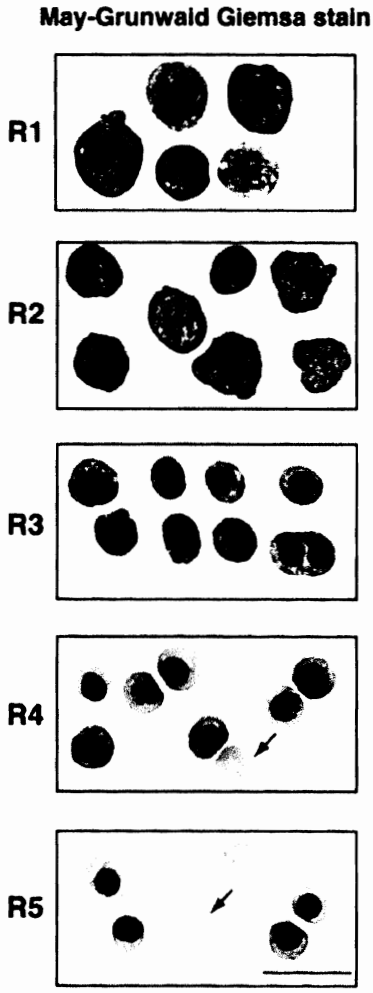

Figure 1: **May-Grunwald Giemsa-stained cytospins from E14.5 fetal liver**. R1 shows mature BFU-Es and CFU-Es. R2 are proerythroblasts and early basophilic erythroblasts. R3 are early and late basophilic erythroblasts. R4 are chromatophilic and orthochromatophilic erythroblasts. R5 are late orthochromatophilic erythroblasts and reticulocytes. Reticulocytes are indicated by arrows (Zhang, 2003).

Table 1. Erythroid Precursors in R1 - R5 Regions Expressing Varying Levels of CD71 and TER119

	R1	R2	R3	R4	R5
Cell	Primitive progenitors and proerythro-blasts	Proerythro-blasts and early basophilic erythroblasts	Early and late basophilic erythroblasts	Chromatophilic and orthochromato-philic erythroblasts	Late orthrochromato-philic erythroblasts and reticulocytes
CD71	MED	HIGH	HIGH	MED	LOW
TER119	LOW	LOW	HIGH	HIGH	HIGH

(Socolovsky, 2001)

Endothelial cell and vasculature development

Essential to embryo survival and primitive erythropoiesis is the development of a vasculature system. This has been proven with early mouse embryonic lethality (E9.5-E10.5) as a consequence of disruption of cardiovascular developmental genes: NCX1, VEGFR1 (Flk-1), Tie2, and EphrinB2 (Wakimoto, 2001; Shalaby, 1995; Gerety, 2002; Dumont, 1994). While EryPs are developing in the yolk sac blood islands, endothelial cells are also developing in the yolk sac. Endothelial cells develop from mesoderm, as do other hematopoietic lineages. A common precursor of erythroid and endothelial cells, called the hemangioblast, is believed to have the ability to differentiate into both endothelial and hematopoietic cells (Choi, 1998). On the other hand, some believe endothelial and erythroid cells are derived from hemogenic endothelium with mesodermal origin. Li et al. (2005) isolated hematopoietic precursor cells from mouse embryos using a combination of CD41, Tie2, and Flk1 markers, and determined that the fraction without CD41 differentiated into endothelial cells while the cells labeling with CD41 became definitive hematopoietic cells. Hematopoietic lineages have been shown to derive from this vascular endothelium surrounding mouse dorsal aorta at E9.5 (Garcia-Porrero, 1998).

Hemoglobin in erythroid cells

While maturation of EryPs and EryDs has been shown to be similar in stage progression, the two populations clearly differ in their globin protein products. Hemoglobin is a tetramer of two α- and two β- noncovalently bound subunits, where each

subunit contains a non-protein heme group inclusive of an iron atom responsible for binding to an oxygen atom. Once oxygen atoms are cooperatively bound to hemoglobin during the act of exchange of oxygen and carbon dioxide in the lungs, oxygen can be transported to various tissues of the body. Mutations in the globin genes result in hemoglobinopathies. These include sickle cell anemia and β-thalassemia, where the former pertains to a defective hemoglobin product and the latter involves a lack of β-globin. These genetic disorders cause significant morbidity and mortality, showing the essential role of hemoglobin in humans.

Sickle cell anemia is an autosomal recessive disorder resulting in the production of hemoglobin S (Hb S). The globin product causes erythroid cells to lose their elasticity and become sickle-shaped due to polymerization of hemoglobin during low oxygen levels or oxygen exchange in the blood. The inability of the erythroid cell to recover its shape and the subsequent decrease in healthy erythroid cells cause anemia, can lead to painful vaso-occlusive crises, acute chest syndrome, stroke and liver failure. The sickle cell shape contributes to vaso-occlusive crises by adhering to vascular endothelium (Frenette, 2007). Sickle-cell anemia affects approximately 72,000 Americans livelihoods and lifespan.

Similarly, β-thalassaemia is an autosomal recessive disorder involving the decreased production of hemoglobin. The defect in the β-globin gene results in α-globin aggregates, due to an improper balance of α- and β- subunits, which can lead to anemia and possibly heart failure. As a result of the globin defect, erythroid cells tend to damage

easily and die earlier than their typical 120-day lifespan in circulation. Currently, bone marrow transplants and blood transfusions are used to treat patients.

β-globin as a model for developmental regulation

During gestation, erythroid cells undergo globin gene switching events, which regulate expression of the β-like-globin proteins. In the case of humans, the first β-like globin to be expressed is ε-globin in embryos, followed by γ-globin in fetuses, and finally β-globin in adults (Figure 2A). The genes are found on chromosome 11 in humans and the proteins have a length of 146 amino acids. In mouse, the β-globin gene cluster is found on chromosome 7 and expression begins with βh1 and ε^y in embryonic blood (EryPs), followed by β-major and β-minor in adult blood (EryDs) (Figure 2B). Upstream of the globin genes is a locus control region (LCR) which is required for enhancement of the activation as well as the appropriate type and timing of globin produced. When the LCR is disrupted, globin expression levels are lowered (Epner, 1998). Within the LCR are several DNase-hypersensitive sites; 5' HSs 1 to 7 in humans and 5' HSs 1 to 6 in mouse (Figure 2A, 2B). These hypersensitive sites can be erythroid and non-erythroid specific (Stamatoyannopoulos, 2002). By providing an enhancement to activation, the LCR acts as a *cis*-acting element for globin genes. It has the capability to give the globin chromatin an "open" configuration to enhance transcription. The LCR has proven to be necessary for *trans*-acting elements such as transcription factors which bind to *cis*-acting elements such as globin promoters, enhancers, and silencers present upstream of individual globin genes. β-globin promoters and the LCR include a critical conserved

sequence, termed the CACCC box, which allows the globin genes to be activated by CACCC-binding nuclear factors such as EKLF.

A. Human β-globin gene (chr 11)

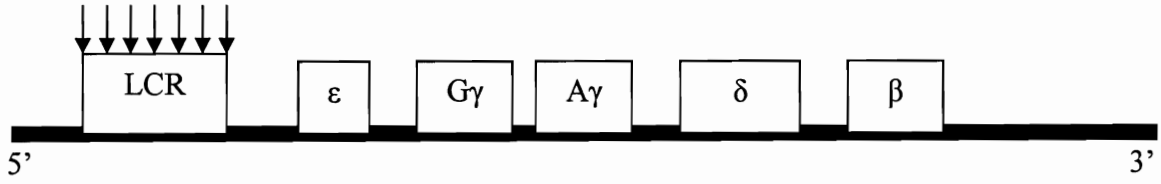

B. Mouse β-globin gene (chr 7)

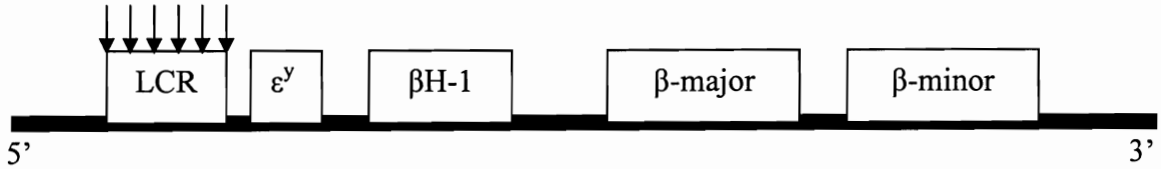

Figure 2: β-globin gene clusters from human and mouse. A) Human. B) Mouse. LCR indicates the locus control region upstream of the genes which is required for enhancement of globin gene activation. Arrows represent DNase hypersensitive elements (5' HS) in the LCR.

Genes required for erythropoiesis

Many genes have been implicated for different stages of erythroid development, which suggests there is temporal and spatial regulation of globin (Orkin, 1997). In studies involving definitive lineage commitment, gene expression shows required genes are "primed" by being transcriptionally active in preparation for differentiation (Ney, 2006). This was shown in studies which looked at expression of various myeloid, megakaryocyte, erythrocyte, monocyte, and granulocyte markers in multipotential progenitors. In another study, cDNA filter arrays were used to track expression of 1200 mouse genes in HSCs and various multipotential cells (Terskikh, 2003). The arrays showed that as the cells differentiated, they lost global gene expression but upregulated lineage-specific gene expression.

As the erythroid progenitors become lineage specific, there are some important genes involved (Figure 3). Erythroid transcription factor, GATA1, and myeloid transcription factor, PU.1, determine whether HSCs differentiate along an erythroid or myeloid lineage (Ney, 2006). GATA1 is expressed as early as in the CFU-E through the polyerythroblast stage. Loss of GATA1 induces apoptosis in erythroid progenitors (Weiss, 1995). It has been shown to repress GATA-2, c-Kit and c-Myc activity, in order to allow erythroid cells to terminally differentiate. GATA2 is required for early hematopoietic development. GATA2 is expressed in the HSC through the polyerythroblast stage, and has been found to be crucial for survival of primitive and definitive progenitors. Further along in development, SCL or Tal1, a helix-loop-helix

transcription factor, regulates embryonic erythropoiesis and is expressed in HSCs. Lmo2 is involved in embryonic erythropoiesis (Ney, 2006).

In definitive erythropoiesis, core-binding factor (CBF) and c-myb are expressed for the differentiation of erythroid cells (Ney, 2006). Several genes have been found to be important in the erythroid proerythroblast. Starting in the CFU-E, erythroid Krüppel-like factor (EKLF or KLF1) and NF-E2 are active and show transcriptional regulation of erythroid cells (Koury, 2002). Erythropoietin and erythropoietin receptor are important for erythroid cell survival (Koury, 2002).

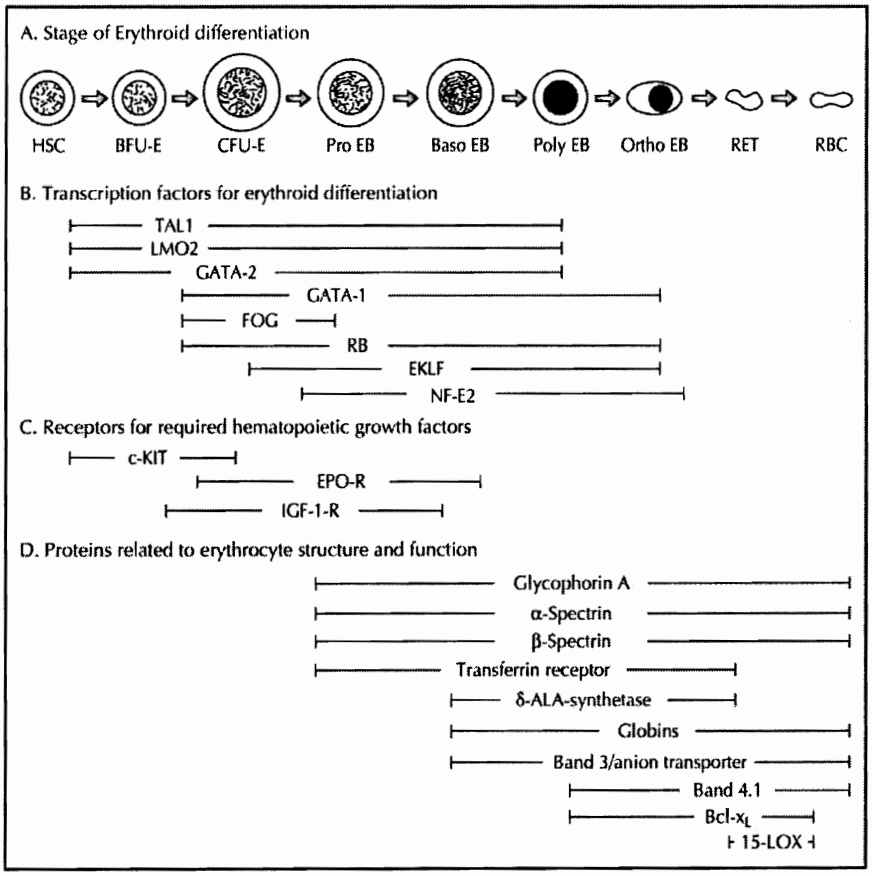

Figure 3: **Gene regulation of erythroid differentiation**. (Koury, 2002). Stages of erythroid differentiation: HSC=hematopoietic stem cell, BFU-E=burst-forming units-erythroid, CFU-E=colony-forming units-erythroid, Pro EB=proerythroblast, Baso EB=basophilic erythroblast, Poly EB=polyerythroblast, Ortho EB=orthoerythroblast, RET=reticulocyte, RBC=red blood cell.

Krüppel-like Factors

Identified based on its homology with *Drosophila* Krüppel protein, EKLF has been studied extensively in mouse erythropoiesis and globin regulation. The discovery has also spurred the establishment of a KLF family inclusive of at least fifteen more factors involved in vascularization, endothelial cells, and terminal differentiation of various other cell types. As a family, all KLF transcription factors contain 3 Cys2/His2 zinc fingers. The zinc finger DNA-binding motif uses a zinc atom to stabilize the 3 cysteine and histidine fingers at the C-terminus of the factor, which subsequently allows the motif to bind to DNA. If EKLF zinc-finger DNA binding domain is disrupted by mutations, the result can be a β-thalassemia-like phenotype in the mouse (Feng, 1998). EKLF can bind to CACCC promoter boxes upstream of globin genes via its zinc-finger domain. The activation level of KLFs is based on the amount and orientation of these CACCC sites found on target genes (Bieker, 1995). EKLF and Krüppel-like factor 2 (LKLF or KLF2) have very similar zinc-finger domains, and are located close to each other in the mouse and human genomes. They were examined in this study.

Role of EKLF in erythropoiesis

EKLF mRNA is found in the chicken in the posterior primitive streak prior to the formation of the blood islands (Chervenak, 2006). In mouse, EKLF is found in primitive streak stage (E7.5) in the yolk sac blood islands as well as the embryo dorsal aortae by E9 and splanchnic mesoderm by E10.5 (Southwood, 1996). EKLF is crucial for definitive cells, as seen in EKLF knockout experiments as described later. EKLF binds to adult β-

globin promoters and LCR DNase hypersensitive sequences, HS 4, HS 3, HS 2, and HS 1 in primitive and definitive cells (Zhou, 2006). By using chromatin immunoprecipitation assays (ChIP), EKLF is bound three-fold more to adult globin promoters in EryD than in EryP progenitors. EKLF is also preferentially bound to embryonic globin promoters in EryPs as compared to EryDs. Analogously, EKLF mRNA is more abundant in EryDs than in EryPs (Chervenak, 2006; Zhou, 2006). This suggests that the erythroid cell embryonic/fetal globin switch to adult globin relies on spatial- and temporal-specific factors.

In prior studies involving single knockout (KO) of EKLF (Perkins, 1995), embryos developed fatal anemia and died by E14.5-16.5. The EKLF gene was knocked out in embryonic stem cells by inserting a neomycin-resistance neo^R cassette interrupting the EKLF zinc-finger DNA binding domain. Once a heterozygous animal was produced, EKLF+/-, they could be bred together to produce EKLF KO animals (EKLF-/-). In knockout studies, EKLF was shown to regulate adult β-major and β-minor globin expression in EryDs (Nuez, 1995; Perkins, 1995). It also affects regulation of EryP hemoglobin metabolism and membrane stability (Hodge, 2006; Drissen, 2005; Nilson, 2006). Although previously reported that EKLF had no effect on embryonic/fetal globin genes, Basu et al. (manuscript under revision) found that E10.5 EKLF KO yolk sac has significantly lower amounts of ε^y and βh-1 globin mRNA than WT. In EKLF KO studies in E12.5 EryDs, erythroid cells accumulated α-globin chains in the form of inclusion or Heinz bodies, due to an imbalanced ratio of α- and β-globin chains (Lim, 1997; Drissen, 2005). Interestingly, the presence of Heinz bodies can be seen in β-thalassemia. By

introducing a human LCR/γ-globin gene into differentiated embryonic stem cells to compensate for the lack of β-globin, the cells were rescued and differentiated into normal, mature adult erythrocytes (Lim, 1997). However, EKLF KO mouse embryos could not be rescued with expression of γ-globin and were still unable to survive through the gestational period (Nilson, 2006). Therefore, EKLF has other gene targets besides the β-globin genes that must be important to embryonic survival and erythroid cells. Spadaccini et al (1998) had previously reported EKLF was not needed for morphological maturation of EryD, which was contradicted by later studies.

Using EKLF KO E12.5 fetal liver EryDs in culture, several gene targets were downregulated; α-hemoglobin stabilizing protein (AHSP), a hemoglobin stability protein, and erythrocyte protein band 4.9 (Epb4.9), an erythrocyte membrane protein (Drissen, 2005; Hodge, 2006). As a result, these erythroid cells were deformed in shape and had wrinkled membrane morphology. This shows the critical role of EKLF in membrane stability and hemoglobin metabolism. Other erythrocyte membrane proteins, β-spectrin and ankyrin, have been shown to be downregulated in similar abnormally-shaped E13.5 EryDs (Nilson, 2006). In the first study of EKLF KO primitive erythroid morphology, E11.5 EKLF KO blood cells had deformed membrane and cell morphology in cytospins, which was similar to E14.5 definitive blood cell morphology (Hodge, 2006). EKLF is involved in regulation of more genes in EryDs than previously believed. The lack of expression of these genes contributes to embryonic lethality as does lack of globin expression.

Although found in progenitors and precursors, EKLF is reported to be primarily required for terminal differentiation of EryDs (Nuez, 1995, Drissen, 2005). This can be seen in flow cytometry studies of E14.5 EKLF KO EryDs double-labeled with TER119 and CD71. E14.5 EKLF KO EryDs expressed lower levels of TER119 and normal levels of CD71 as compared to WT (Hodge, 2006). Interestingly, EKLF KO E14.5 EryDs also showed transferrin receptor 1 (TfR1) mRNA was expressed at significantly lower (~10-fold) levels. At some posttranscriptional timepoint before E14.5, low levels of TfR1 mRNA are compensated to assay normal CD71 expression as seen by flow cytometry. E12.5 EKLF KO fetal liver (Drissen, 2005) and E14.5 EKLF KO fetal liver (Hodge, 2006) were labeled for annexin V, an early marker for apoptotic cells, and showed the same expression as seen in WT and EKLF+/- genotypes. Therefore, the lack of EKLF was not causing apoptosis in these EryDs.

To examine the EryP expression of TER119 and CD71 markers, flow cytometry of E11.5 erythroid cells was performed (Hodge, 2006). However, as previously shown by Fraser et al (2007), E11.5 blood may contain EryDs in spite of a large fraction being EryPs. Additionally, at E11.5, EKLF+/- genotype generated intermediate levels of TER119 while EKLF-/- genotype showed even lower levels when both were compared to WT (no data for EKLF+/- at E14.5). It can be inferred that the number of expressed alleles (+/+, +/-, -/-), directly correlates to the expression pattern of the TER119 cell marker on erythroid cells. EKLF clearly has a role in cell surface expression and maturation of EryPs and EryDs.

Role of KLF2 in development

KLF2 was discovered using the EKLF zinc-finger domain as a hybridization probe; the two KLFs are about 90% similar in their zinc-finger domain (Anderson, 1995). The EKLF and KLF2 genes are located 6 Mb apart on human chromosome 19 and mouse chromosome 8. EKLF and KLF2 bind to similar CACCC elements, which suggest a relationship between the two factors. KLF2 expression has been found in, but is not limited to: lung tissue, endothelial cells, adipocytes, red blood cell precursors, epithelial cells in yolk sac, and T lymphocytes. Using in situ hybridization, KLF2 was discovered to be expressed as early as E8.5 in endothelial cells in all vasculature in the murine embryo; by E14.5, KLF2 was expressed in the lung buds, vertebral column and developing bone of the head and ribs (Lee, 2006; Kuo, 1997). Through microarray expression profiling in human umbilical vein endothelial cells (HUVEC), KLF2 has been implicated in cell migration, vasomotor function, inflammation, and hemostasis (Dekker, 2006). In thymocytes, KLF2 KO has resulted in incompetent T-lymphocyte migration (Carlson, 2006). It also has been implicated in T-cell cell cycle and apoptosis regulation. KLF2 expression has also been shown to be activated in cultured and in vivo endothelial cells by fluid shear forces or proinflammatory stimuli (Lee, 2006, Suzuki, 2005, Wang, 2006).

KLF2 KO mice were produced by inserting a vector into the target KLF2 gene of embryonic stem cells (Kuo, 1997; Wani, 1998). When homologously recombined with the endogenous KLF2 gene, the resulting deletion removed the promoter region, transcription activation domain, and some of the DNA binding domain. This deleted

gene cannot be transcribed (Wani, 1998). On the other hand, Kuo et al (1997) inserted a PGK-*neomycin* cassette to replace the entire KLF2 gene. The cells containing the vector were selected, harvested, and screened for KLF2 and subsequently injected into blastocysts and then female mice. The KLF2 KO mouse died in utero between E12.5-E14.5 due to hemorrhaging. At E11.5, KLF2 KO embryos appeared to have normal vasculogenesis and angiogenesis (Kuo, 1997). In the E12.5 KLF2 KO dorsal aorta, endothelial cells were abnormally cuboidal in shape, but not apoptotic (Kuo, 1997). Before embryonic lethality, the lack of KLF2 expression caused vascular endothelial cells to become defective and to lead to intraembryonic hemorrhaging. Histologically, tunica media around umbilical vessels were thinner than normal with disorganization and reduced number of smooth muscle cells in E12.5 embryos (Kuo, 1997). Also, extracellular matrix of the tunica media was significantly reduced in these embryos. Tunica media and the smooth muscle cells are derived from the mesenchymal cells differentiating adjacent to the endothelial cells surrounding developing vessels. Importantly, loss of KLF2 did not have an effect on several vascular growth factors which are crucial to blood vessel formation (Kuo, 1997; Lee, 2006). In endothelial cells from E12.5 KLF2 KO, crucial genes Tie1, Tie2, PDGF-B, and HB-EGF were expressed normally, as also seen with TGF-β which is required for smooth muscle cells (Kuo, 1997; Lee, 2006). Conditional knockout of KLF2 in endothelial cells also lead embryos to heart failure and death at E14.5 (Lee, 2006). Heart failure could be due to KLF2 direct effects on vascular endothelial cells.

While endothelial cells have been the large focus of KLF2 KO studies, erythroid cells have also been studied due to the DNA-binding motif similarity between KLF2 and EKLF. In vitro, cultured E11.5 KLF2 KO fetal liver definitive erythroid cells differed little from cultured WT fetal liver cells. Also, E12.5 blood smears showed no morphological differences between KLF2 KO and WT (Kuo, 1997). However, Wani et al. observed in E11.5 KLF2 KO blood smears that a large number of nucleated primitive erythroid cells rather than mature enucleated blood cells as seen in WT. This could be due to the specific method the KLF2 gene was targeted and knocked out in the Wani model. Basu et al (2006), using the Wani model, observed changes in E10.5 KLF2 KO erythroid cells. The E10.5 KLF2 KO mouse yolk sac, primarily primitive erythroid cells, contained two-fold more irregularly-shaped erythroid cells than in wildtype (WT). Expression of ε^y and βh-1 globin mRNA was 2-fold lower than WT littermates. β-major and β-minor globin expression did not differ in WT, KLF2+/-, and KLF2-/- at E12.5. TUNEL assay showed that the KLF2 KO embryonic yolk sac contained a significantly higher percentage (~5-fold) of apoptotic erythroid cells.

Simultaneous ablation of EKLF and KLF2 in E10.5 mouse embryo

Thus far, research on EKLF and KLF2 factors show that they are essential transcriptional regulators of early development in erythroid and endothelial cell lineages. They could potentially have overlapping roles in globin regulation, which is tied closely to embryonic and definitive erythropoiesis. To examine this hypothesis, mice in this lab were generated with null alleles of both EKLF and KLF2 on the same chromosomal

homolog. Due to the proximity of the two genes on chromosome 8, over 100 pups were tested for the recombination event before two mice were generated with the correct genotype. Subsequent crosses were performed with wildtype mice to establish more recombinant double heterozygotes (EKLF+/-KLF2+/-). EKLF+/-KLF2+/- mice were then crossed to produce double KO (EKLF-/-KLF2-/-) embryos.

When examined at E10.5, the double KO embryos were discovered to be anemic with pale aortae. From whole mount images, forebrain and hindbrain size was decreased in 80% of embryos. This phenotype was also found in E12.5 KLF2 KO embryos (Kuo, 1997). In E10.5 EKLF-/-KLF2-/- yolk sacs, levels of ε^y and βh-1 globin mRNA were one-fifth of WT, as well as significantly lower than in either EKLF KO or KLF2 KO. Double KO levels of glycophorin A (GPA) mRNA were normal when compared to WT, which suggested that primitive erythropoiesis was taking place in some capacity. Both KLFs are clearly involved in the regulation of the embryonic globin genes, as simultaneous ablation of both can greatly lower their expression levels. This confirms the compensatory functions of the two KLFs.

This lead to the question of what events were occurring in the double KO erythroid cells to cause drastic change in globin levels. Additionally, if globin expression levels appeared significantly decreased, then it was hypothesized that the double KO embryos would die at an earlier day of gestation than the single KOs. One hypothesis was that EKLF-/-KLF2-/- primitive blood cells matured less well than single KO. With flow cytometry techniques, problems seen in erythroblast differentiation could potentially be quantified, as previously done for EKLF-/- cells. It was also important to determine

whether circulation of erythroid cells was normal. In addition, it would be important to analyze both erythroid and endothelial cells. Another hypothesis was that if EKLF targets erythroid cell regulation and KLF2 targets endothelial cell development, then both types of cells would likely be affected in the double KO.

This study was designed to examine the developmental effects and cell morphology of E9.5 double KO embryos. At E9.5, it has been shown that about 97% of the blood consists of primitive erythroid cells (EryPs) (Fraser, 2007). By performing these experiments at E9.5, it was possible to study the roles of EKLF and KLF2 in primitive erythropoiesis.

The model may prove useful in the future as gene therapy becomes more of a reality in the clinic. EKLF and KLF2 gene targets such as erythroid membrane proteins, globin, or endothelial cells can point to ways to recover deficient levels of globin or aid in the treatment of β-thalassemia or sickle cell anemia. Ultimately, primitive erythropoiesis is a model of developmental design; it has the potential to illuminate other differentiation programs also starting from stem cells.

CHAPTER 2

MATERIALS AND METHODS

Generation of Mice

EKLF +/- (KLF1+/-) mice were acquired from Jackson Labs (USA) as made by Perkins et al. (1995) and KLF2 +/- mice were obtained from Wani et al. (1998). As previously described in those studies, the EKLF and KLF2 alleles were each knocked out or made inoperative on one chromosome. The two genotypes, EKLF +/- and KLF2 +/- were bred together until a recombination event occurred during which the knockout alleles of EKLF and KLF2 would be on the same chromosomal homolog, expressed as EKLF +/- KLF2 +/- genotype (Basu et al, manuscript under revision). Matings were then set up by against normal FVB/N mice to generate additional EKLF+/-KLF2+/- mice. EKLF+/- mice were bred to generate EKLF-/- embryos, and KLF2+/- mice were bred to generate KLF2-/- embryos. Once heterozygous mice (EKLF+/- KLF2 +/-; EKLF+/-; KLF2+/-) were at the appropriate age of 6-8 weeks-old and weight of at least 23.0 grams, the mice were mated to examine their progeny. Peanuts were given to mice to encourage weight gain. Vaginal openings of female mice were examined every day after their dark cycle ended. Once a vaginal plug was discovered, the time of gestation was established as day 0.5 and the female mouse was isolated from the male. The female mice were monitored and dissected nine (9) days following presence of plug, hence E9.5 embryos.

The predicted genotypes and percentages obtained from the double heterozygous matings were 25% EKLF+/+ KLF2+/+, 50% EKLF+/- KLF2+/-, and 25% EKLF-/- KLF2-/-. Similarly, both EKLF+/- and KLF2+/- matings produced 25% WT, 50% heterozygous (EKLF+/- or KLF2+/-), and 25% knockout (EKLF-/- or KLF2-/-). Recombination events could occur at about 2% frequency, as seen in previous matings.

Genotyping

In order to determine the genotypes of embryos and mice, PCR was used. Primers were used to distinguish the wildtype and deleted EKLF and KLF2 alleles. Mouse ear punches were digested in digestion buffer (50mM KCl, 10mM Tris HCL (pH 8.5), 40mM $MgCl_2$, 0.45% Nonidet P40 lysis buffer, and 0.45% Tween 20) and 1μg/μl proteinase K (serine protease that cleaves at the carboxylic ends of aliphatic, aromatic, and hydrophobic amino acids) and incubated overnight at 60 °C. Proteinase K was inactivated by heating samples for 2 10-minute cycles at 95 °C. In between heating steps, samples were zip-spun in an Eppendorf 5415C micro-centrifuge (Eppendorf, Westbury, NY) for a few seconds. Samples were stored at 20°C until ready for polymerase chain reaction. A PCR grand mix was prepared with 10X PCR buffer (200 mM Tris-HCl-pH 8.4 and 500 mM KCl), 0.2 mM dNTP mixture, 1.5 mM $MgCl_2$, 0.5 μM of each normal and knockout primer, and subsequently stored at 20 °C. Primers used in this case were *forward* and *reverse* normal and *forward* and *reverse* knockout (Table 2). For the PCR reaction, *Taq* DNA Polymerase (0.04 U/ μl), 1.75 μg/μl/reaction RNase A, and molecular grade H_2O was added to the PCR. 24 μl of PCR mix and 1 μl of cellular extract were

added to 8-strip PCR tubes. Previously confirmed tissue samples were used as EKLF and KLF2 positive controls and duplicates of samples were included in each PCR run. Duplicates were performed to confirm results. For negative controls, a sample was run containing 1 µl of H_2O in PCR grand mix in order to test for contamination in PCR mix or H_2O. PCR tubes were initially denatured at 94 °C for 3 min, then 35 cycles at 94 °C for 40 sec, 58 °C for 45 sec, and 72 °C for 1 min 15 sec, and finally ended with an extension step of 72 °C for 5 min. PCR samples were run on 2% agarose gels made with 100 ml of 1X TAE buffer (10X TAE: 2M Tris base, 10mM Glacial Acetic Acid, 10mM EDTA pH=8, and deionized H_20), 2.0 grams of Seakem LE agarose (Cambrex), and 0.00075% ethidium bromide. The solution was heated in an Erlenmeyer flask in a household microwave oven (Sharp Electronics Corp) for 3-4 minutes. Once the flask's contents stopped bubbling and ethidium bromide had been incorporated, the agarose was poured into a medium size gel casting tray with two 20-lane gel combs inserted at the top and halfway point of the gel. Upon solidifying, the gel apparatus was filled with 1X TAE buffer. Each well was loaded with 10 µl of PCR product mixed with 1 µl of loading buffer. Electrophoresis was performed at 95 volts for 0.5 hr for EKLF gels and 1.5-2.0 hrs for KLF2 gels. Gels were imaged and analyzed using an Alpha Innotech fluorochrome imager camera and software (San Leandro, CA). For EKLF gels, +/- bands were present at about 200 bp and 400 bp where the knockout band is 400 bp, while in KLF2 gels, +/- bands were closer in proximity at 380 bp and 422 bp where the latter is the knockout allele.

TABLE 2: EKLF and KLF2 primers

	Forward normal	Reverse normal	Forward knockout	Reverse knockout
EKLF	5'-CCTGAGCTACTTAGTGAGATCC-3'	5'-TTCTTCTCCCATCTCTAACCC-3'	5'-AGAGGCTATTCGGCTATGACTG-3'	5'-TTCGTCCAGATCATCCTGATC-3'
KLF2	5'-TTGTTTAGGTCCTCATCCGTGCCG-3'	5'-TTGCCGTCCTTTGCCACTTTCG-3'	5'-TGCTTACAACCTCCTAAATGTTCTGA-3'	5'-CCTACCCGCTTCCATTGCTC-3'

Microdissection of E9.5 embryos for sectioning

Nine days following the presence of the vaginal plug, the pregnant female mice were anesthetized with 2.5% Avertin (10g of tribomoethyl alcohol in 10 ml tertiary amyl alcohol) at 0.015 ml/g body weight and sacrificed by cervical dislocation. The embryos were dissected out into 1X PBS and 30mm Petri dishes using watchmaker forceps and surgical scissors under an Olympus SZ2-ILST microscope at 20X magnification [eye piece objective-WHSZ10X-H/22, objective-110AL2X-2]. Whole mount images were taken with an Olympus Q-Color 3 camera and QCapture 2.81.0 software (Quantitative Imaging Corporation). Yolk sac and embryo were carefully separated from each other and a piece of the embryo tail was used for genotyping by PCR. Remaining yolk sacs and embryos were placed in fixative (2% paraformaldehyde and 2.5% glutaraldehyde) overnight in 2 dram tooled neck glass vials. The next day, tissues were rinsed three times and left in Millonig's buffer (pH=7.2-7.4, Appendix-Solutions) where they were stable until embedding.

Plastic embedding of yolk sacs and embryos

Samples were processed by passing them 3 times through a 5-minute wash of Millonig's buffer and osmicating for 40 minutes in 1% Osmium tetroxide at 4 °C. At room temperature, they were dehydrated with 30%, 40%, 50%, 60%, and 70% ethanol for 5 minutes each and 80%, 95%, 95%, 100%, and 100% ethanol for 10 minutes each. Tissues were then placed in a 50:50 mix of 100% ethanol and propylene oxide for 5 minutes, followed by washing twice for 10-minutes with propylene oxide, and finally incubated overnight in a 50:50 mix of eponate 12 and propylene oxide. The tissues were embedded the next day after 4 hours in 100% eponate 12 resin. The plastic blocks were placed in a 55 °C oven for 3 days to allow the eponate 12 resin to polymerize.

Sectioning for light and electron microscopy

Semi-thick sections of yolk sac and embryos were cut at 2 μm and 6 μm, respectively, on a Leica LKB 2128 Ultramicrotome. Sections were placed in series on Superfrost©/Plus microscope slides (Fisher Scientific), heated gently on a hot plate and stained with 1% Sodium borate, 0.1% Methylene Blue, 0.1% Azure Blue, and 0.1% Toluidine Blue. Microscopic analysis was performed with a Nikon Optiphot microscope fitted with an Olympus DP70 digital camera.

For electron microscopy, sections were cut at 100 nm with a LKB 2128 Ultratome and stained with 5% Uranyl Acetate and Reynold's Lead Citrate. Images were taken on the JEOL JEM-1230 TEM (JEOL (U.S.A.), INC., Peabody, MA) with the Gatan Ultrascan 4000 digital camera (Gatan Inc., Pleasanton, CA).

Microdissection of E9.5 embryos for flow cytometry analysis

Each uterine implantation site containing an E9.5 embryo was dissected in FACS buffer [1x PBS + 5% Fetal Bovine Serum] to isolate the embryo and visceral yolk sac. After removing maternal tissues, the yolk sacs and embryos were rinsed in FACS buffer and FACS buffer + heparin (0.2U/ml) and finally placed in 500 µl of FACS buffer + heparin in a 24-well plate and the large vessels were cut. Embryonic blood was allowed to drain for 10 minutes and subsequently collected in a 1.5 ml Eppendorf tube. An additional 500 µl of FACS buffer was used to rinse the well. Blood was centrifuged for 5 minutes at 3000 rpm and the clear supernatant was removed. The blood cells were resuspended in 100 µl of FACS buffer.

Antibodies and flow cytometry

Cells were double-labeled with PE-conjugated anti-TER119 and FITC-conjugated anti-CD71 (transferrin receptor) (eBiosciences, San Diego, CA) and incubated in the dark at 4° C for 20 minutes. Cells were spun and washed once more and resuspended in 100µl FACS buffer in preparation for flow cytometry. Samples were gently pushed through 35 um nylon mesh into flow cytometry tubes and run on an EPICS Elite ESP Flow Cytometer (Coulter, Fullerton, CA) at low rate. Level II and III beads of the EPICS intensity standard kit were used for calibration of fluorescent intensity (Coulter). Once forward scatter and side scatter plots were produced, a gate was drawn around the primitive erythroid population. Based on single-stained samples of PE-anti-TER119 and FITC-anti-CD71, five gates R1-R5 could be drawn. R1 and R2 were drawn as TER119

negative and R3, R4, and R5 were drawn as TER119, according to Zhang et al. (2003) and Fraser et al. (2007).

Cytospins

Samples containing 5,000 to 20,000 cells were sorted into 100 µl of media in plastic cytospin buckets. Cells were spun on a SCA0081 cytospin (Shandon Southern) with filter cards (Shandon) at 20,000 rpm for 5 minutes onto Superfrost©/Plus (Fisher) glass slides. Slides were then air dried, fixed with methanol for 3 minutes, and Giemsa stained for 10 minutes (Sigma Aldrich, St. Louis, MO). Once washed, the slides were analyzed on a Nikon Optiphot microscope and Olympus DP70 digital camera.

CHAPTER 3

RESULTS

EKLF-/-KLF2-/- embryonic lethality

EKLF/KLF2 double knockout (KO) mice died by E11.5. At E9.5, E10.5, and E11.5 progeny were statistically examined to determine if the predicted ratio of genotypes resulted from heterozygous [EKLF+/-KLF2+/- *x* EKLF+/-KLF2+/-] matings. Expected genotypes are WT (EKLF+/+KLF+/+), heterozygous (EKLF+/-KLF2+/-), and double KO (EKLF-/-KLF2-/-) in a 1:2:1 ratio. At E9.5, the progeny had the expected distribution of genotypes. Among forty-one embryos dissected at E9.5, fourteen live embryos were genotyped to be EKLF-/-KLF2-/-, which proved not to be statistically different from expected as the χ-square value was 0.8234 (Table 3). A χ-square value>5.99 was taken as significantly different from the expected distribution. In gross morphology, E9.5 EKLF-/-KLF2-/- whole mount images (Figure 4B) did not look different from WT (Figure 4A) embryos and yolk sacs. At E10.5, the sixty-five genotyped embryos were at the expected ratio of WT, heterozygous, and KO with a χ-square value of 0.143. Whole mount images of E10.5 WT yolk sacs surrounding embryos had normal vasculature and color (Figure 4C), while EKLF-/-KLF2-/- yolk sacs appeared pale (Figure 4D). WT and EKLF-/-KLF2-/- yolk sacs were then removed without severing the vitelline and umbilical vessels in order to show embryo vasculature

(Figure 4E and 4F). In E10.5 EKLF-/-KLF2-/- embryos and yolk sacs, vasculature appeared devoid of normal amounts of red blood cells. At E11.5, out of twenty-three live embryos, no EKLF-/-KLF2-/- embryos were found. This proved to be a statistically significant difference from the expected distribution, with a χ-square value of 6.817. At E11.5, although ten EKLF-/-KLF2-/- embryos were observed, they were all dead and in the process of resorption back into maternal tissue. Therefore, the expected number of EKLF-/-KLF2-/- conceptuses was observed, but they do not survive to E11.5.

Table 3: Number of Live Embryos Observed from Matings of EKLF+/-KLF2+/- mice

Days of Gestation	WT	EKLF+/-KLF2+/-	EKLF-/-KLF2-/-
E9.5	9	18	14
E10.5	14	34	17
E11.5*	6 (2)	17	0 (10)

* means significantly different distribution of embryos than expected according to χ-square analysis
( ) means number of resorbed, dead embryos

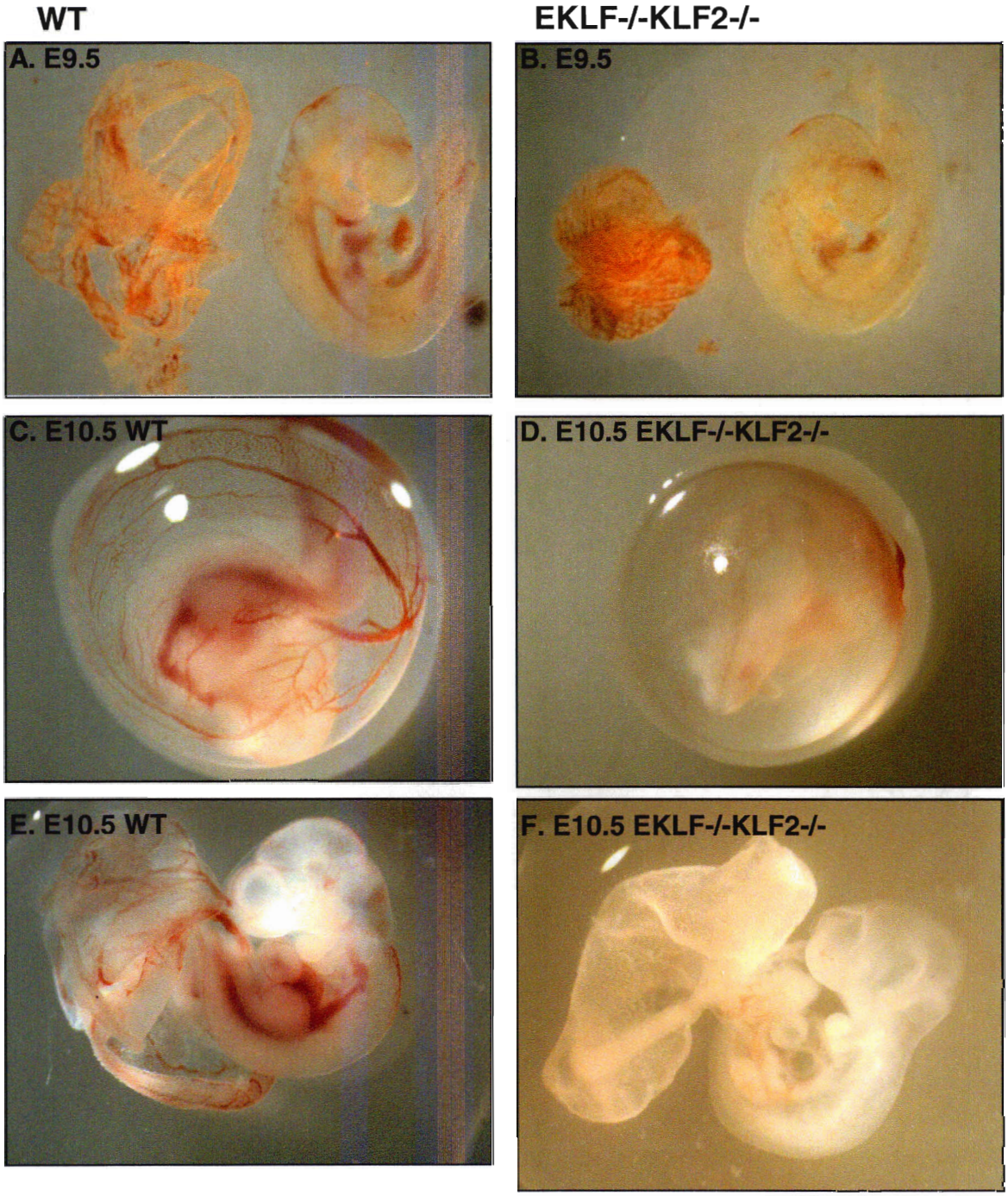

Figure 4A-F: Whole Mount Images of E9.5 and E10.5 WT and EKLF-/-KLF2-/- Embryos. WT embryos in the left panel. Double KO embryos in the right panel. A) E9.5 WT embryo. 16x magnification. B) E9.5 double KO embryo. 16x mag. C) E10.5 WT embryo within yolk sac. 20x mag. D) E10.5 double KO embryo within yolk sac. 20x mag. E) E10.5 WT embryo with yolk sac peeled off. 20x mag. F) E10.5 double KO embryo with yolk sac peeled off. 20x mag.

Abnormal morphology of erythroid, endothelial, and mesothelial cells in E9.5 EKLF-/-KLF2-/- yolk sac

EKLF-/-KLF2-/- double KO yolk sacs and embryos were compared to WT and KLF2 KO. Tissues were fixed in 2% paraformaldehyde/2.5% glutaraldehyde overnight and subsequently rinsed in Millonig's buffer. After embedding in epoxy plastic, semi-thick sections were cut and stained with Toluidine Blue. Interestingly, at the light microscopic level, it was possible to identify abnormalities in erythroid, endothelial, and mesothelial cells of the yolk sac in the double KO embryos (Figure 5A-D). Three different yolk sacs for each genotype were used to confirm histological findings. In both WT and KLF2-/- (KLF2 KO) yolk sac, the attenuated endothelial and mesothelial cell layers contained normal, squamous cells (Figure 5A). The erythroid cells were round and regular in shape. This was in sharp contrast to the double KO yolk sacs, which showed a thickening of the combined endothelial and mesothelial cell layers (Figure 5B). Four measurements of the space between the two cell layers (not inclusive of endothelial or mesothelial cells) were taken of one yolk sac section from each genotype. The average width of the double KO endothelial and mesothelial cell layers was 10.75μm. This is statistically different from averages from WT (p-value=0.0165) of 1.75μm and KLF2 KO (p-value=0.0208) of 2.25μm (Table 4). EKLF-/-KLF2-/- erythroid cells appeared irregular in shape with the presence of protruding cytoplasmic extensions compared to the regular shape of the WT and KLF2 KO (Figure 5A, B, C). Partial cross-sections of erythroid cell cytoplasmic extensions frequently were present in the blood vessels of the double KO yolk sac. Endothelial and mesothelial cells were not squamous but ballooned into the blood vessel and extraembryonic coelom, respectively. In the double KO yolk

sacs, some epithelial cells appeared to form ingrowths (Figure 5D) resulting in a deep ciliated epithelial-lined invagination protruding into the extraembryonic coelom. Consequently, epithelial cells formed invaginations resulting in a new lumen or cavity where it is not usually found. Examining two sections from three yolk sacs per genotype, instances of epithelial ingrowths were averaged per yolk sac and subsequently averaged per genotype. In the first double KO yolk sac, two sections each had three epithelial invaginations. In the second yolk sac, one section had three while the second section had two invaginations. Out of two sections of the third yolk sac, only one section had one invagination present. These morphological anomalies occurred on average two times in double KO yolk sac and zero times in WT and KLF2 KO (Table 4). Except for these rare invaginations, the epithelial cells lining the yolk sac cavity appeared normal and therefore were not involved in histological abnormalities.

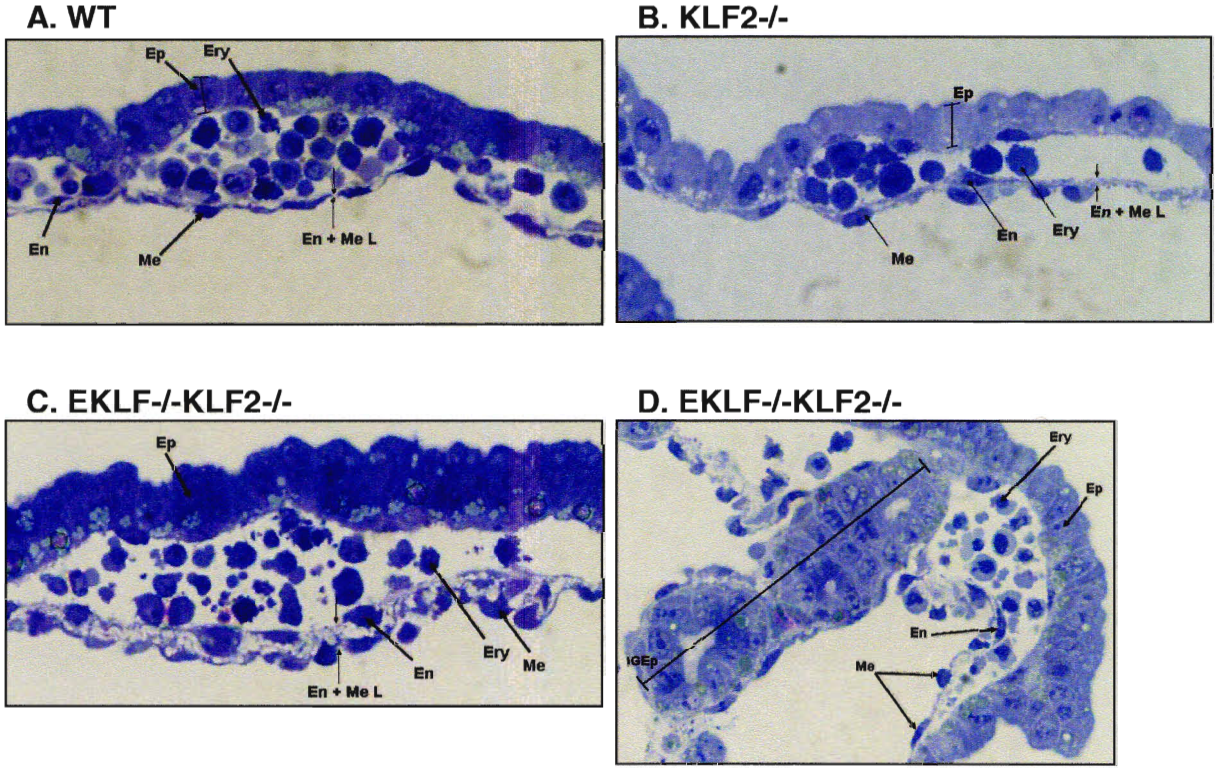

Figure 5A-D: Light micrographs of E9.5 yolk sac at 400X. A) Wildtype yolk sac. Squamous endothelial (En) and mesothelial (Me) cell layers are tightly apposed. Erythroid (Ery) and epithelial (Epi) cells are normal. B) KLF2 single KO yolk sac. Ery, En, Me, and Ep cells appear normal. C) EKLF-/-KLF2-/- KO yolk sac with irregularly shaped erythroid (Ery), bulbous mesothelial and endothelial cells, and increased intercellular space between En and Me cell layers. Ery show cytoplasmic protrusions. D) Presence of epithelial ingrowth (IGEp) in double KO. Double KO yolk sacs appear to have a disturbance in development of blood cells and blood vessels, not seen in the single KO of KLF2 or WT.

Table 4: Quantification of Other Abnormal Morphology in the E9.5 Yolk Sac

Genotype	Average Epithelial Ingrowths per Yolk Sac	Average Distance Between En + Me Layer
	n=3	n=3
WT	0	1.75 μm
KLF2-/-	0	2.25 μm
EKLF-/-KLF2-/-	2	10.75 μm *

* means significantly different from WT and KLF2 at p-value<0.025

EKLF-/-KLF2-/- E9.5 yolk sacs contain more abnormal cells than KLF2-/- or WT

In order to quantify the morphological results, we used criteria to discern abnormal from normal erythroid, endothelial, and mesothelial cells. The criterion used to designate erythroid cells as abnormal was that at least 25% of the cell volume protruded from the cell, resulting in an irregular shape. Partial cross-sections of cells were not counted. Abnormal endothelial and mesothelial cells were counted as abnormal if they appeared non-squamous and bloated into the blood vessel or extraembryonic space, respectively. One plastic section from each of the three different yolk sacs per genotype was used to analyze erythroid, endothelial, and mesothelial cells. The percentage of abnormal cells and standard deviation was calculated and Student's unpaired, two-tailed t-test was used to identify significant differences (Figure 6). A p-value<0.025 was considered significant. In WT sections, approximately 380 (n=380) erythroid cells were counted and 2.9% appeared abnormal. In EKLF/KLF2 KO sections, 737 (n=737) erythroid cells were counted and 54.2% were abnormal, which is 19-fold higher than WT with a significant p-value of 0.001. In KLF2 KO sections, 280 (n=280) cells were counted with 1.2% abnormal; the percentage of abnormal erythroid cells in KLF2 KO and WT were not significantly different from each other. Similarly, the percentages of abnormal endothelial cells in EKLF/KLF2 KO (n=445 total cells) were 32-fold higher and significantly different from those in WT (n=148 total cells) with a p-value of 0.0108. EKLF/KLF2 KO abnormal endothelial cells were 5-fold higher in percentage from those found in KLF2 KO (n=181 total cells) and the results gave a p-value of 0.0239. Abnormal endothelial cells were further quantified based on which side of the blood

vessel they lay on, either next to the epithelial cell layer or the mesothelial cell layer. In EKLF/KLF2 KO, 60.7% of endothelial cells located next to the mesothelial cell layer were abnormal, while a significantly lower percentage (1.2%, p-value=0.0029) of endothelial cells found on the epithelial cell side were abnormal (Figure 7). There was a 4-fold higher percentage of abnormal mesothelial cells in EKLF/KLF2 KO (n=1154 cells, p-value=0.002) than in KLF2 KO (n=320 cells) and WT (n=330 cells) (Figure 6). Therefore, EKLF/KLF2 double KO proved to be significantly different from both WT and KLF2 KO yolk sacs. Taken together, there are significantly higher percentages of abnormal erythroid, endothelial, and mesothelial cells in the yolk sacs of the double KO than in single KO and WT.

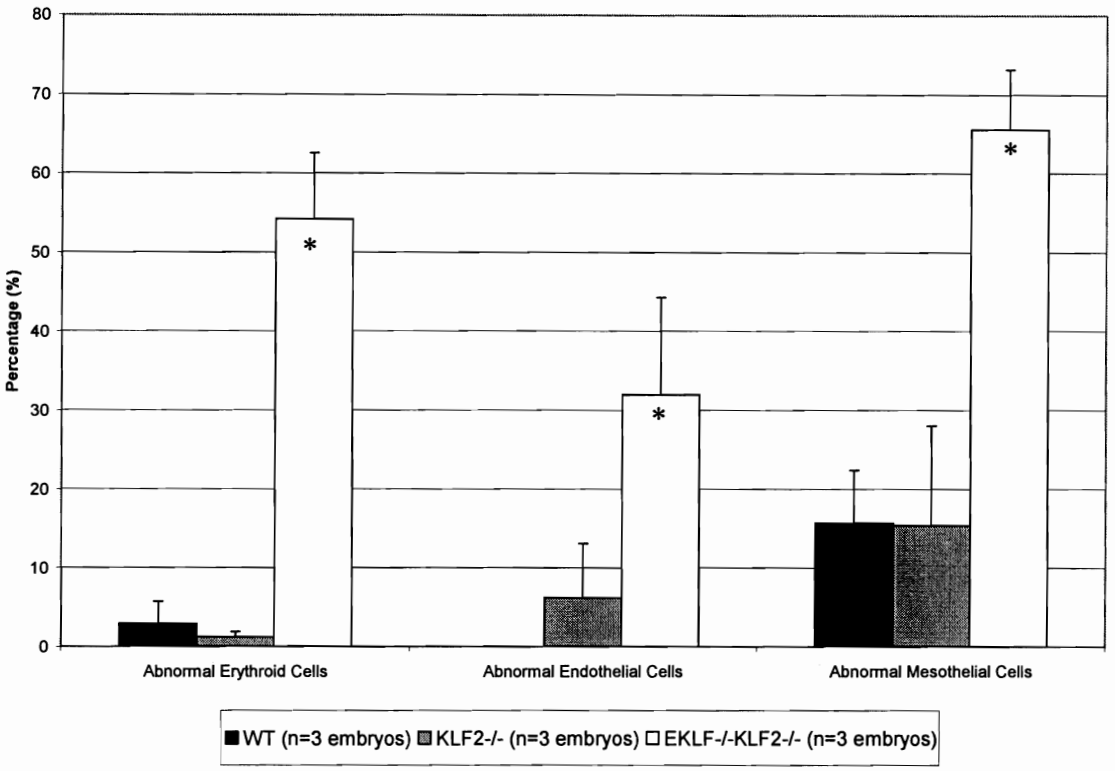

Figure 6: Quantification of abnormal erythroid, endothelial, and mesothelial cells in E9.5 yolk sac. Average percentages of abnormal Ery, En, and Me cells in WT, KLF2 KO and EKLF-/-KLF2-/- KO yolk sacs were calculated. Genotype and total erythroid cells counted: WT (*n*=380 cells), KLF2 KO (*n*=280), and EKLF/KLF2 KO (*n*=740 cells). Genotype and total endothelial cells counted: WT (*n*=150), KLF2 KO (*n*=180 cells), and EKLF/KLF2 KO (*n*=445 cells). Genotype and total mesothelial cells counted: WT (*n*=330 cells), KLF2 KO (*n*=320 cells), and EKLF/KLF2 KO (*n*=1150 cells). ["*n*" represents the number of cells used to determine the percentages from 3 yolk sac sections of each genotype. "n" signifies the number of mice yolk sacs were counted for each genotype.] Error bars are standard deviation from the mean. "*" means significantly different from WT and KLF2 at p-value<0.025.

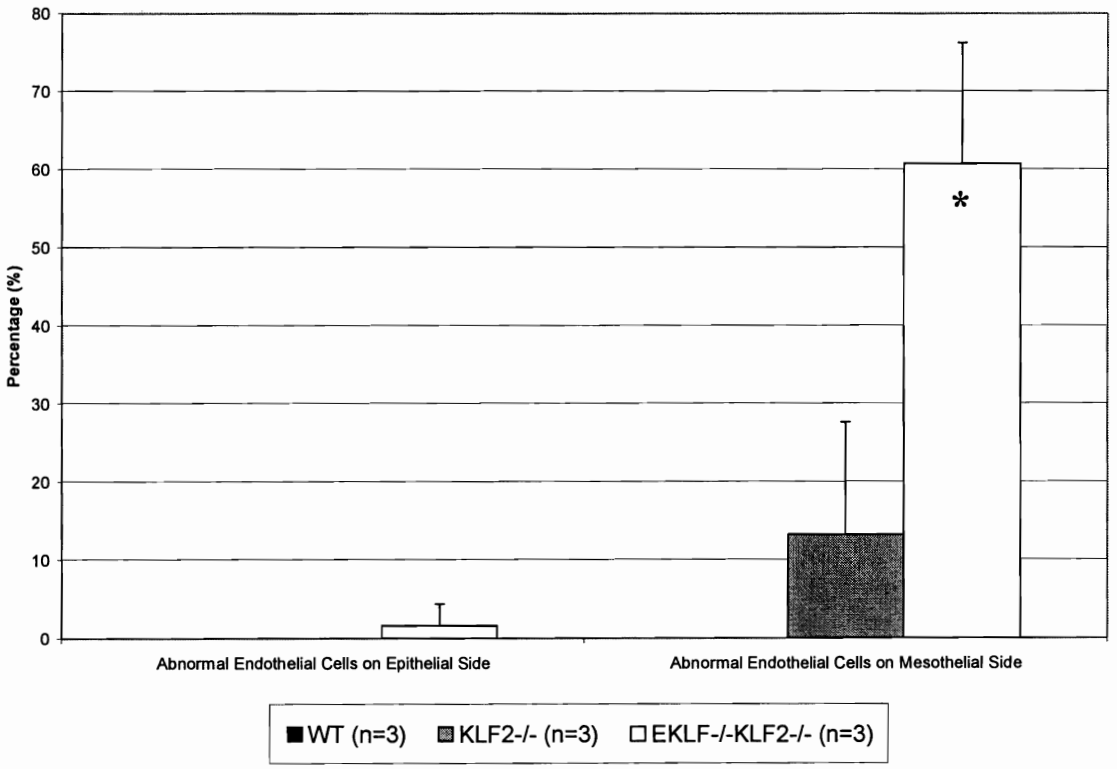

Figure 7: Quantification of abnormal endothelial cells in E9.5 yolk sac based on location in WT, KLF2 KO, and EKLF/KLF2 double KO. Three different yolk sacs were used to quantify abnormal endothelial cells. Abnormal endothelial cells were counted based on bloated morphology and placement-either on epithelial side or mesothelial side of the blood vessel in yolk sacs. No abnormal endothelial cells were found in WT yolk sacs, hence no bars are present. Additionally, no abnormal endothelial cells were observed on the epithelial side of the KLF2 KO yolk sac. "*" means significantly different from WT and KLF2 KO at p-value<0.025. Error bars are standard deviation.

Electron microscopy reveals abnormal erythroid, endothelial, and mesothelial cells in EKLF-/-KLF2-/- E9.5 yolk sacs

Electron microscopy was used to further examine the phenotypic differences in the yolk sac between the WT and EKLF/KLF2 KO genotypes. In the WT yolk sac (Figure 8A), endothelial and mesothelial cells were squamous and tightly apposed on the extraembryonic coelom side of the yolk sac. In the EKLF/KLF2 KO yolk sac (Figure 8B), the intercellular space between the two cell layers appeared disturbed with innumerable cytoplasmic protrusions from the endothelial and mesothelial cell layers. The mesothelial cells appeared to balloon into the extraembryonic coelom as was also observed using light microscopy. A representative erythroid cell from a double KO (Figure 8C) also has an interrupted morphology as evidenced by approximately 25% of the cytoplasm displaced from the cell. Epithelial ingrowths were present which produced a lumen as evidenced by microvilli-lined invaginations (Figure 8D). E10.5 KLF2-/- yolk sac was previously examined using electron microscopy (Basu, 2005), and most primitive erythrocytes were found to have cytoplasmic protrusions. However, there were no abnormalities of endothelial or mesothelial cells observed, at E10.5, and no erythroid abnormalities were observed at the light microscopic level in E9.5 KLF2 KO erythroid cells (Figure 5B). At this higher level of magnification, yolk sac problems confirm light microscopy findings.

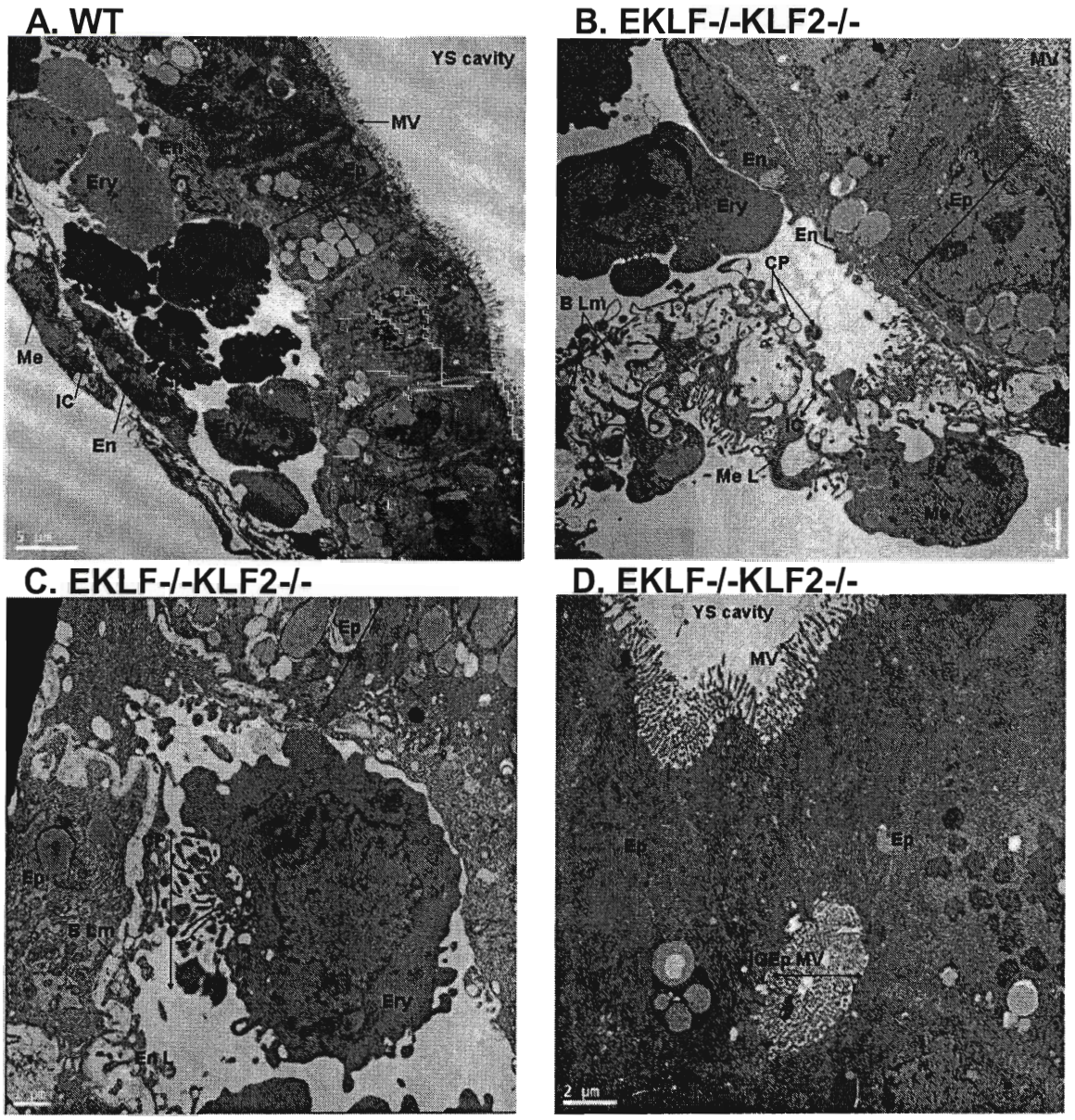

Figure 8A-D: Representative electron micrographs of E9 yolk sacs. A) 6000 mag. Wildtype yolk sac showing mesothelial cell layer (Me), endothelial layer (En), erythroid cells (Ery), epithelial cells (Ep) and its microvilli (MV), as well as normal intercellular space between the Me and En layer (IC). B) 6000 mag. EKLF-/-KLF2-/- yolk sac showing an increased IC, abnormal cytoplasmic projections (CP) from endothelial layer, discontinuous basal lamina (B Lm), and bulbous mesothelial cells (Me). C) 16,000 mag. Additional anomaly seen in the EKLF-/-KLF2-/- erythroid cell at this level. Basal lamina (B Lm) appears detached and cytoplasm projects (CP) from the erythroid cell. D) 16,000 mag. EKLF-/-KLF2-/- epithelial cells. Microvilli (MV) are seen lining an invagination of the epithelium that has formed.

Histological analysis of embryos

Abnormal endothelial cells were observed in EKLF-/-KLF2-/- yolk sacs at E9.5; the next step was to determine if this endothelial cell phenotype occurred in the embryo. Therefore, the dorsal aorta of the embryo was examined. By E8.5 in the mouse embryo, the dorsal aorta forms a pair of vessels, which are the first and the predominant blood vessel in the body. The dorsal aortae also serve as a transient site of erythropoiesis between the yolk sac and the fetal liver. At E9.5, the WT dorsal aorta (Figure 9A) showed regularly shaped erythroid cells contained within a blood vessel consisting of a single layer of endothelial cells, which in turn also apposes an area of mesenchymal cells. Mesenchymal cells are similar to the mesothelial cells in the yolk sac in that they are both mesodermal in origin and provide support around forming blood vessels. In the dorsal aortae of EKLF/KLF2 KO embryos (Figure 9B), erythroid cells again appear irregular and associated with extra cytoplasm. The space between endothelial and mesenchymal cells was also thickened in double KO, showing a loss in integrity of their cell layer contact. Dorsal aorta of E9.5 double KO showed similar features as seen in the double KO E9.5 yolk sac. However, only one double KO dorsal aorta has been thoroughly examined thus far, and more analysis will need to be performed in order to determine if this is a representative finding.

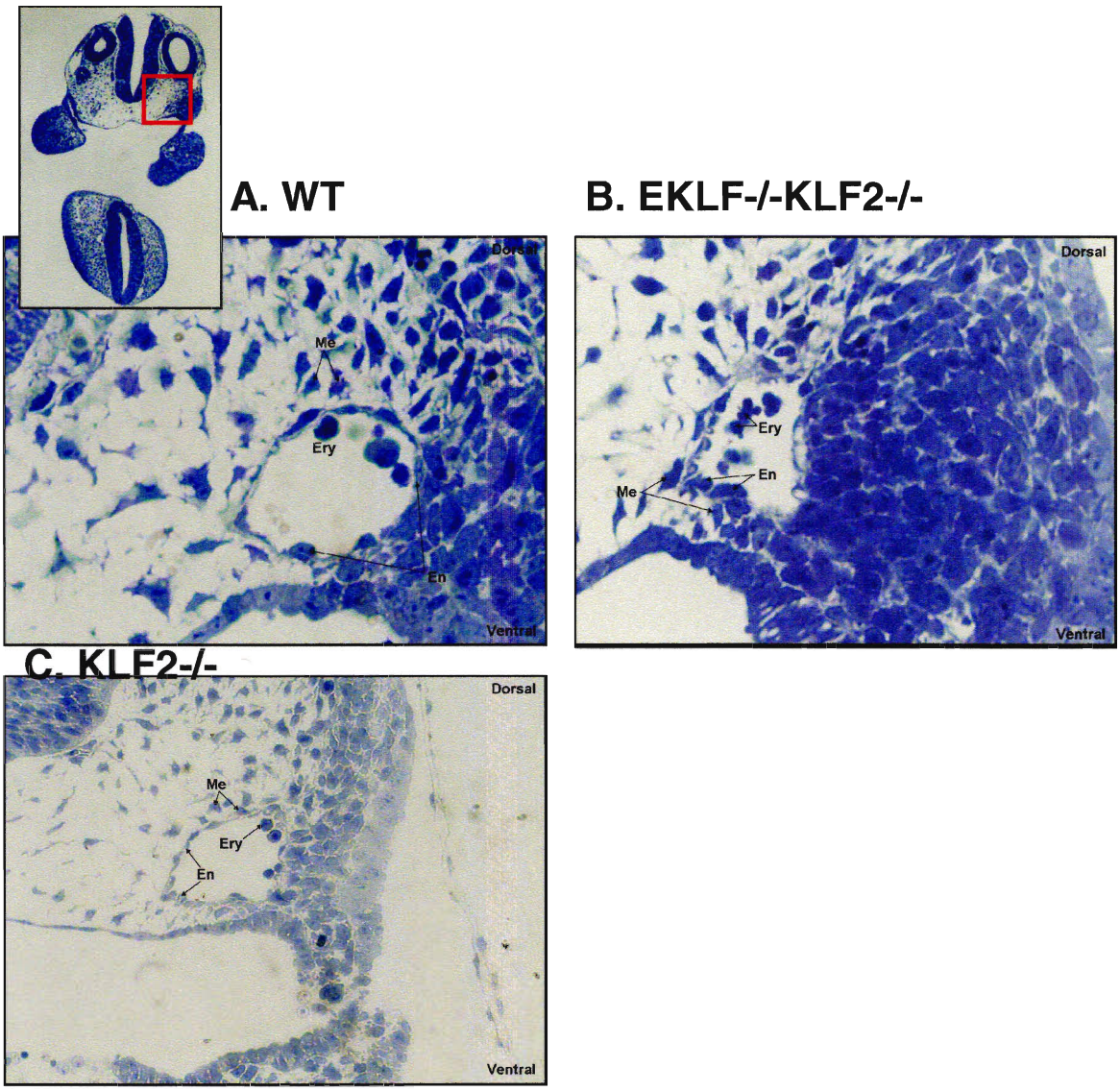

Figure 9A-C: Light micrographs (400X and 200X) of E9.5 embryo sections with focus on dorsal aorta. Dorsal and ventral orientations are as indicated. Two embryos of each genotype were examined and representative micrographs are shown. A) Inset: E9.5 WT embryo section at 100X. Red frame: area magnified in next image. WT dorsal aorta. WT shows tight, compact endothelial layer (En L) as well as normal shaped erythroid cells (Ery) and squamous endothelial cells (En). Endothelial cells have normal interactions with mesenchymal cells (Me). B) 200X mag. EKLF-/-KLF2-/- dorsal aorta shows a disturbed endothelial cell layer. Erythroid cells have cytoplasmic projections. Erythroid and endothelial cells in the embryo, as in the yolk sac, are abnormal. Mesenchymal cell interactions with endothelial cells show disorganization. C) 200X mag. KLF2-/- dorsal aorta appears normal with regular erythroid and endothelial cells. Endothelial cell layer surrounding the dorsal aorta is compact and tight as in WT. Mesenchymal and endothelial cell interaction is normal.

Primitive erythroid cells are apparently larger in size in EKLF-/- and EKLF-/-KLF2-/- than in KLF2-/- and WT

Flow cytometry was used to determine the presence of the cell surface markers, TER119 and transferrin receptor (CD71), on primitive erythroid cells. When comparing seven different genotypes, TER119/CD71 histoplots were used to examine maturational changes. If TER119 and CD71 expression were lowered compared to E9.5 WT blood, it would signify a change in erythroid cell maturation or differentiation. Based on TER119 and CD71 staining intensity, five regions, R1-R5, were drawn in order to separate the primitive cell populations by erythroblast precursor stage; R1 being the more immature cells while progressing towards mature cells in R5. At least eight different blood samples were used to corroborate the phenotypes generated by crosses, EKLF+/- *x* EKLF+/- and EKLF+/-KLF2+/- *x* EKLF+/-KLF2+/-. For the KLF2+/- *x* KLF2+/- matings, only one KLF2-/- blood sample has been obtained. The number of erythroid cells from the yolk sac and embryo ranged from 28,000 to 588,000. When maternal blood cells were plotted on forward scatter and side scatter plots (FS/SSC) to compare size and granulation (Figure 10A), primitive erythroid cells were larger in size than maternal red blood cells, as expected. In the E9.5 double KO FS/SSC plot (Figure 10D), primitive erythroid cells are apparently increased in size as seen in the upper shift of the targeted population compared to WT or EKLF-/- primitive erythroid cells (Figure 10B and C). Based on the FS/SSC plot, a gate was drawn to isolate the primitive erythroid cells with minimal maternal blood contamination, (ranging from 5,000 to 80,000) to be sorted for cytospins. Additionally, this population was further analyzed based on double-staining with FITC-anti-CD71 and PE-anti-TER119.

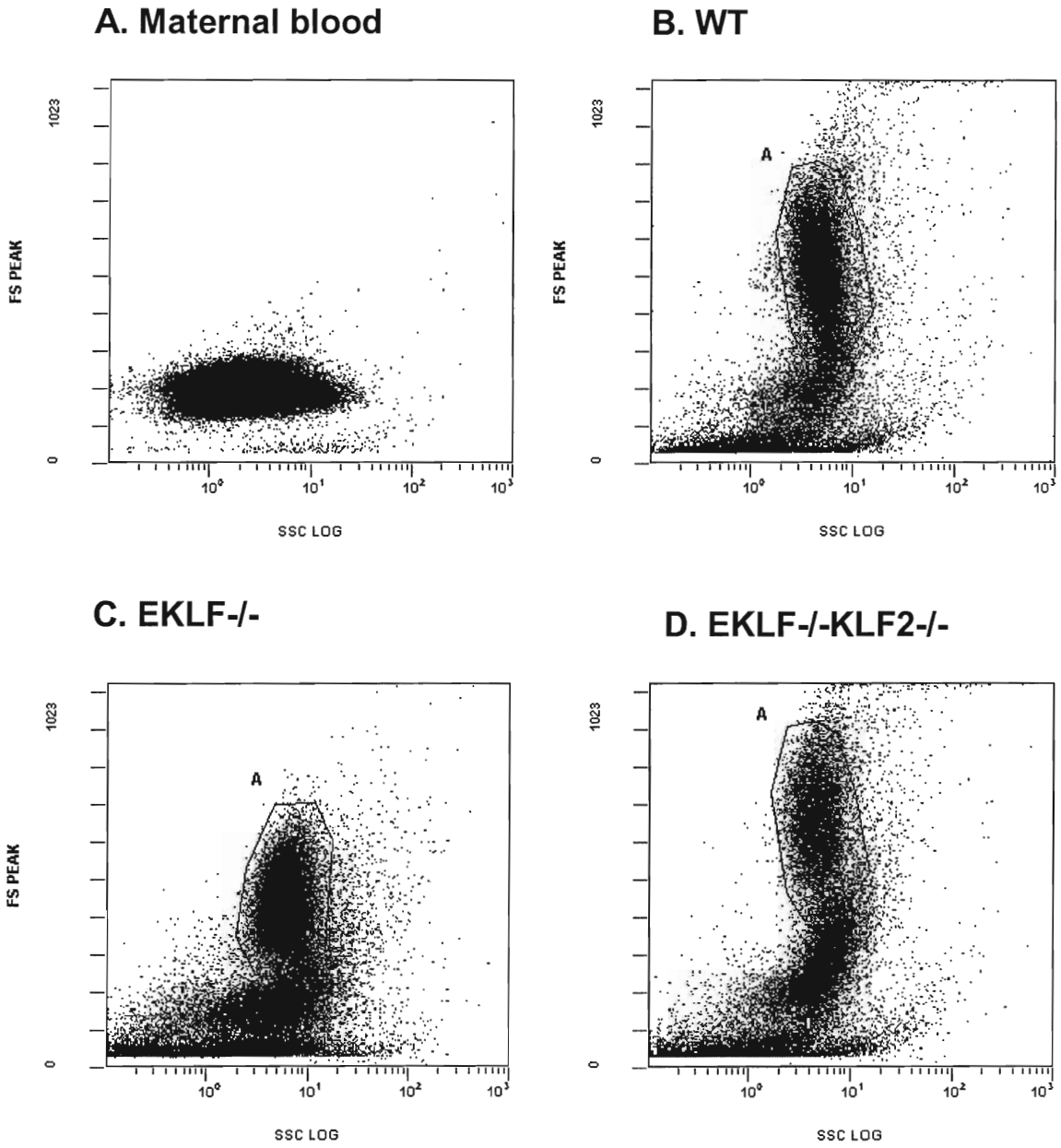

Figure 10A-D: **Representative forward/side scatter histoplots of maternal blood and E9.5 embryonic blood.** "A" region marks the gate used for cell sorting primitive erythroid cells for cytospins as well as for further analysis based on TER-119 and transferrin receptor markers. A) Maternal blood. Histoplot shows maternal blood does not contaminate "A" gate. B) WT. C) EKLF-/- KO genotype. D) EKLF-/-KLF2-/- double KO shows population of primitive erythroid cells has shifted higher on forward scatter.

Cytospins of E9.5 EKLF-/- and EKLF-/-KLF2-/- primitive erythroid cells indicate morphology changes

In observing cytospins, WT erythroid cells appeared round in shape with normal staining in the nuclei (Figure 11A). WT differed little from EKLF+/-KLF+/- or KLF2-/- in erythroid shapes (Figure 11B and C). EKLF-/- erythroid cells have morphological abnormalities in the cell membrane and possibly cytoplasm. Abnormal protrusions were noted in many of EKLF-/- erythroid cells (Figure 11D). Compared to EKLF-/-, EKLF-/-KLF2-/- double KO erythroid cells showed a more progressively perturbed and lengthened shape (Figure 11E). At least eight different blood samples were used to corroborate each genotype: WT, EKLF+/-KLF2+/-, EKLF-/-, and EKLF-/-KLF2-/-. Only one KLF2-/- blood sample was obtained from KLF2 matings.

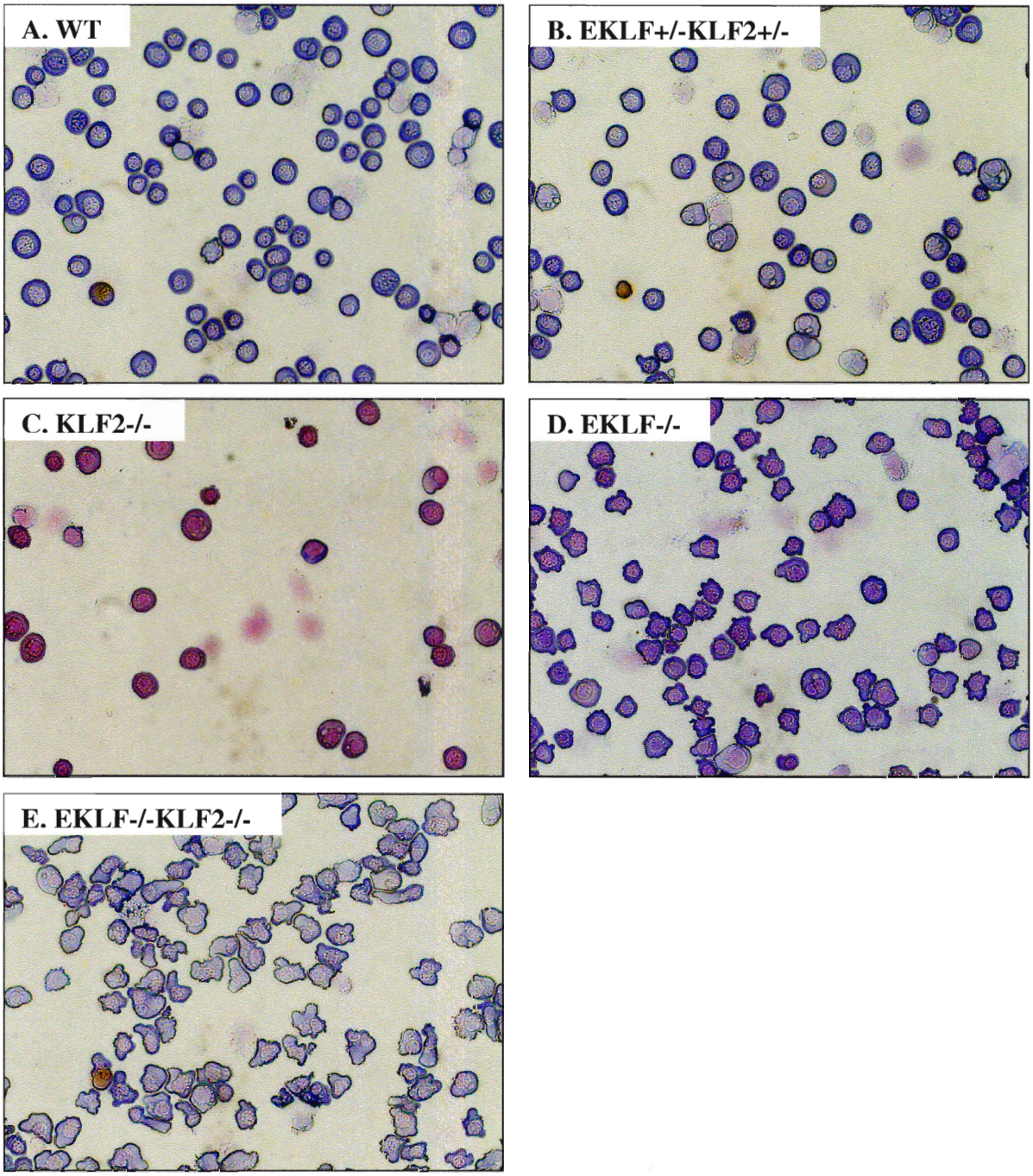

Figure 11A-E: Flow Cytometry Cytospins (400x) of Giemsa-stained E9.5 primitive erythroid cells. A) WT erythroid cells are regular (n=32 embryos). B) EKLF+/-KLF2+/- double heterozygous erythroid cells appear normal (n=9 embryos). C) KLF2-/- erythroid cells appear like WT (n=1 embryo). D) EKLF-/- erythroid cells appear irregular with cytoplasmic protrusions (n=10 embryos). E) EKLF-/-KLF2-/- erythroid cells look most irregular in the double KO with abnormal elongation and protrusions of cell shape.

Quantification of abnormal primitive erythroid cells in EKLF-/- and EKLF-/-KLF2-/- cytospins

Using embryonic blood cytospins from three E9.5 embryos for each genotype, quantification of the percentage of abnormal erythroid cells was carried out to determine the extent of altered morphology. At least 500 cells from one embryo were counted for each genotype examined. Criterion for abnormal erythroid cells was that at least 25% of the cytoplasm was part of a cell protrusion or elongation. Blebbing-type cytoplasmic extensions of less than 25% of the cell volume were not counted as abnormal as these were seen in WT erythroid cells. Averages and standard deviations were calculated for each genotype and Student's t-test was performed, and a $p<0.0025$ was considered significant (Figure 12). The percentage of abnormal erythroid cells in EKLF+/- and KLF2+/- embryos was not significantly different from WT. The percentages of abnormal erythroid cells in EKLF-/- and EKLF-/-KLF2-/- double KO were significantly greater than WT. However, in comparing EKLF-/- to EKLF-/-KLF2-/-, erythroid cells were not significantly different (p-value=0.6088). When using different criteria (i.e. percentage of elongated cells), there were significantly more abnormal cells in EKLF-/-KLF2-/- than EKLF-/- (data not shown). This indicates that based on the criteria used, different results could be obtained. In most cases, using criteria based on specific structures such as cytoplasmic blebbing, nuclear polarization, and pleiomorphic cytoplasm may be more conclusive. Statistical analysis could not be performed with KLF2-/- genotype because of insufficient sample size. Taken together, these results show a significantly abnormal erythroid cell phenotype in both EKLF KO and double KO E9.5 embryos.

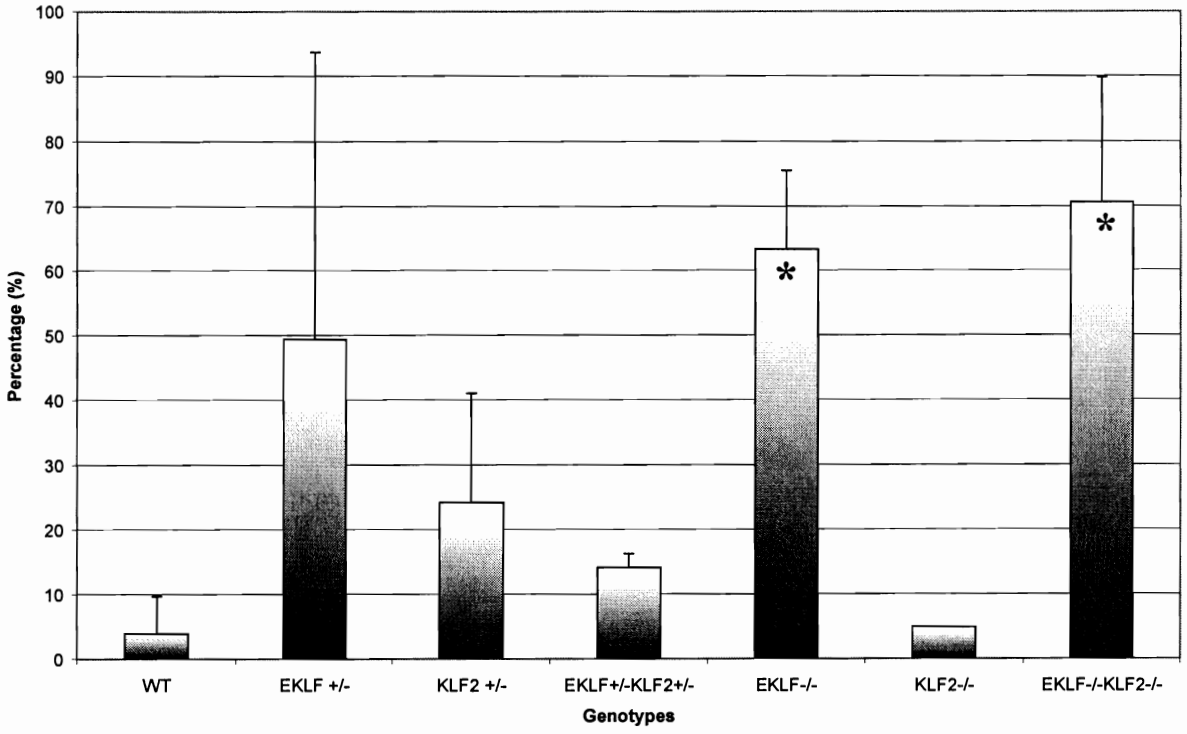

Figure 12: **Abnormal Cell Count from E9.5 Primitive Erythroid Cytospins**. For each genotype, 3 different embryos were chosen at random for quantification of abnormal cells. At least *n*=500 cells were counted for each genotype and an abnormal average percentage was determined, with the exception of KLF2-/- (n=1). Error bars represent standard deviation from the mean. ["*" means genotype significantly different from WT.]

TER119/CD71 staining of E9.5 EKLF-/- and EKLF-/-KLF2-/- primitive erythroid cells indicate maturational abnormalities

When primitive erythroid cells were plotted against TER119 and CD71 markers, it was possible to determine their maturational stage. Using PE-anti-TER119 only and FITC-anti-CD71 only labeled E9.5 WT blood as controls, gates were set for R1 ($CD71^{med}TER119^{low}$), R2 ($CD71^{high}TER119^{low}$), R3 ($CD71^{high}TER119^{high}$), R4 ($CD71^{med}TER119^{high}$), and R5 ($CD71^{low}TER119^{high}$) (Table 1). Based on where the double-labeled cells fell on histoplots, the percentage of cells in the R1-R5 regions could be quantified (Figure 13). Average percentages of cells within each gate were calculated among the seven genotypes: WT (EKLF+/+KLF2+/+), EKLF+/-, KLF2+/-, EKLF+/-KLF2+/- (Figure 14A) and EKLF-/-, KLF2-/-, EFLF-/-KLF2-/- (Figure 14B). Average percentages from WT (n=32) gates R1-R5 came to a total of 92.3% (Table 5); the remaining percentage of cells were present on the histoplots but did not fall in gates R1-R5. Subsequently, the other genotypes were corrected to this total percentage in order to normalize the raw averages for more accurate comparison (Table 5). A second population could be seen in most FITC/PE histoplots from all genotypes, which plotted below the primary population usually straddling the R1 and R4/R5 regions. It is not certain how the labeling of this secondary subpopulation of cells influences this analysis or what is exactly contained in this population. WT (n=32 blood samples) showed the majority, 77%, of labeled cells were in R3 (Figure 14A and B). KLF2+/- (Figure 13C, 14A) and KLF2-/- (Figure 13F, 14B) plotted most similarly to WT. Percentages of cells were considered significantly lower in R1 and R2 in KLF2+/- when compared to WT. (No statistical analysis for KLF2-/-) EKLF+/-KLF2+/- heterozygous (n=9 blood

samples) (Figure 13D, 14A) showed most of the labeled cells are in R2, which also resembles EKLF+/- (n=23) averages (Figure 13B, 14A). In EKLF/KLF2 double heterozygous, the percentage of cells in R2 and R3 were significantly higher and lower, respectively, from those in WT. In R1 and R2 of EKLF+/-, percentages were significantly higher than WT, while in R3, EKLF+/- percentages were significantly lower from WT (Table 5). The blood from EKLF-/- (n=10) (Figure 13E, 14B) showed that almost the same percentage of double-labeled cells were in R1 and R2, but then sharply decreased to the lowest levels found for R3 among all genotypes. For regions R1 and R2, EKLF-/- had significantly higher percentages of cells when compared to WT. In R3, EKLF-/- had significantly lower percentages of cells than WT (Table 5). Finally, in the EKLF-/-KLF2-/- double KO (n=8), about the same percentage of cells were labeled in regions R1-R3 and R4-R5. Percentages in R1, R2, and R4 were significantly higher than those found in WT, while those found in R3 were significantly lower than WT (Figure 14B, Table 5). Surprisingly, double KO percentages in regions R4 and R5 were the highest found among these seven genotypes; this was unexpected since it was hypothesized that the double KO cells would be more immature rather than mature. While progression towards R4 and R5 is an indication of increased maturation, the double KO cells do not appear to be more mature then those in WT. EKLF-/-KLF2-/- was significantly higher than EKLF-/- in two of these regions: R3 and R4 (Table 5). Overall, double KO cells showed the most altered cell morphology with an unexpected cell surface expression neither definitively more nor less mature.

An additional comparison between WT and EKLF-/-KLF2-/- sorted primitive erythroid cells showed significant differences between mean TER119 and CD71 staining intensity (Figure 15). Taking the mean measurement of marker staining for two embryos of WT and three of EKLF-/-KLF2-/-, the latter showed a significant decrease in both CD71 and TER119 staining. However, when EKLF-/- (n=3) was compared to EKLF-/-KLF2-/- (n=3), sorted primitive cells were 1.5-fold lower in TER119 and CD71 mean fluorescence intensity. While results were significantly different by a p-value<0.025, it is uncertain how different EKLF-/- are from EKLF-/-KLF2-/- primitive erythroid cells.

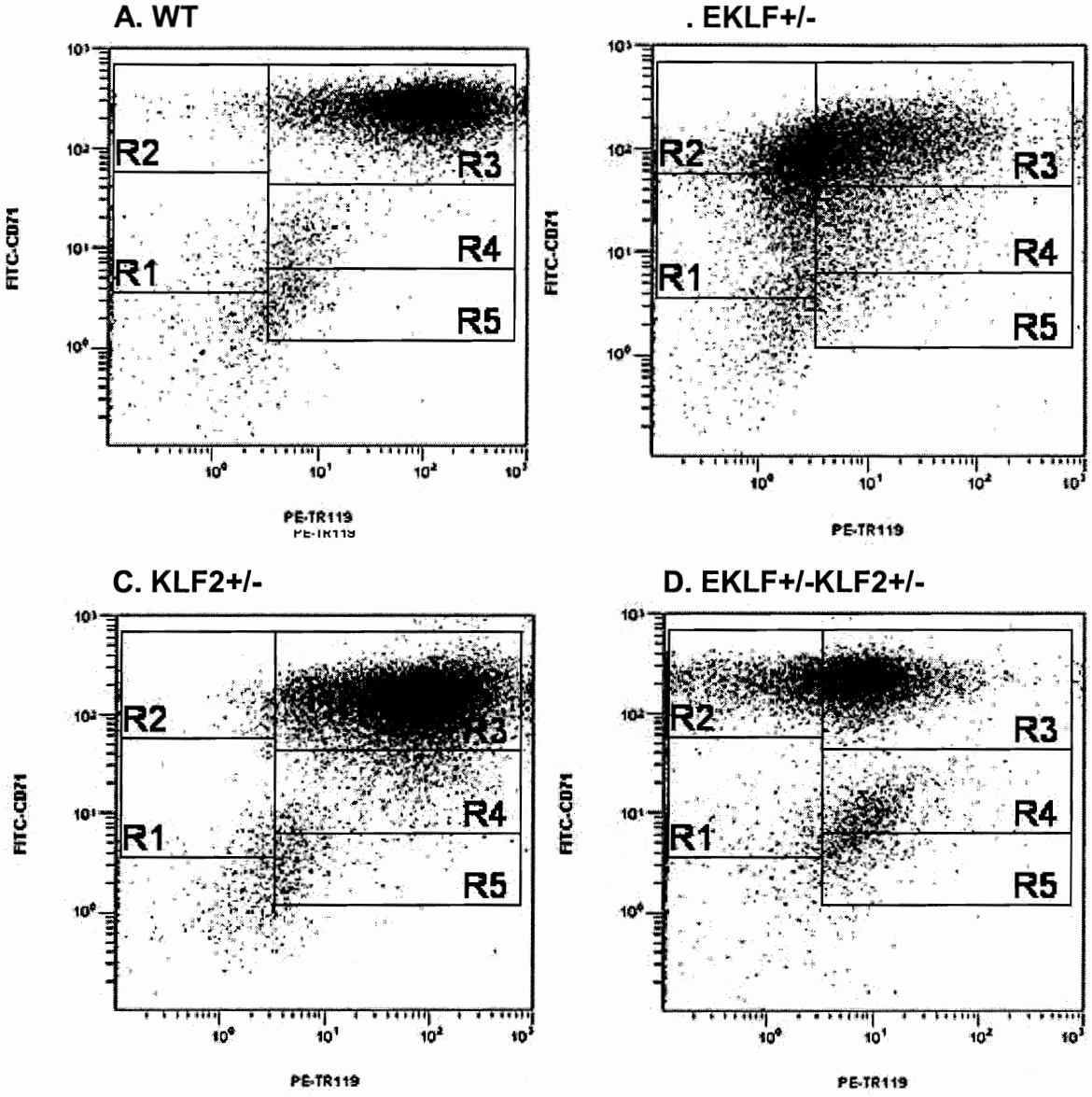
A. WT
. EKLF+/-
C. KLF2+/-
D. EKLF+/-KLF2+/-
R1
R2
R3
R4
R5
FITC-CD71
PE-TR119

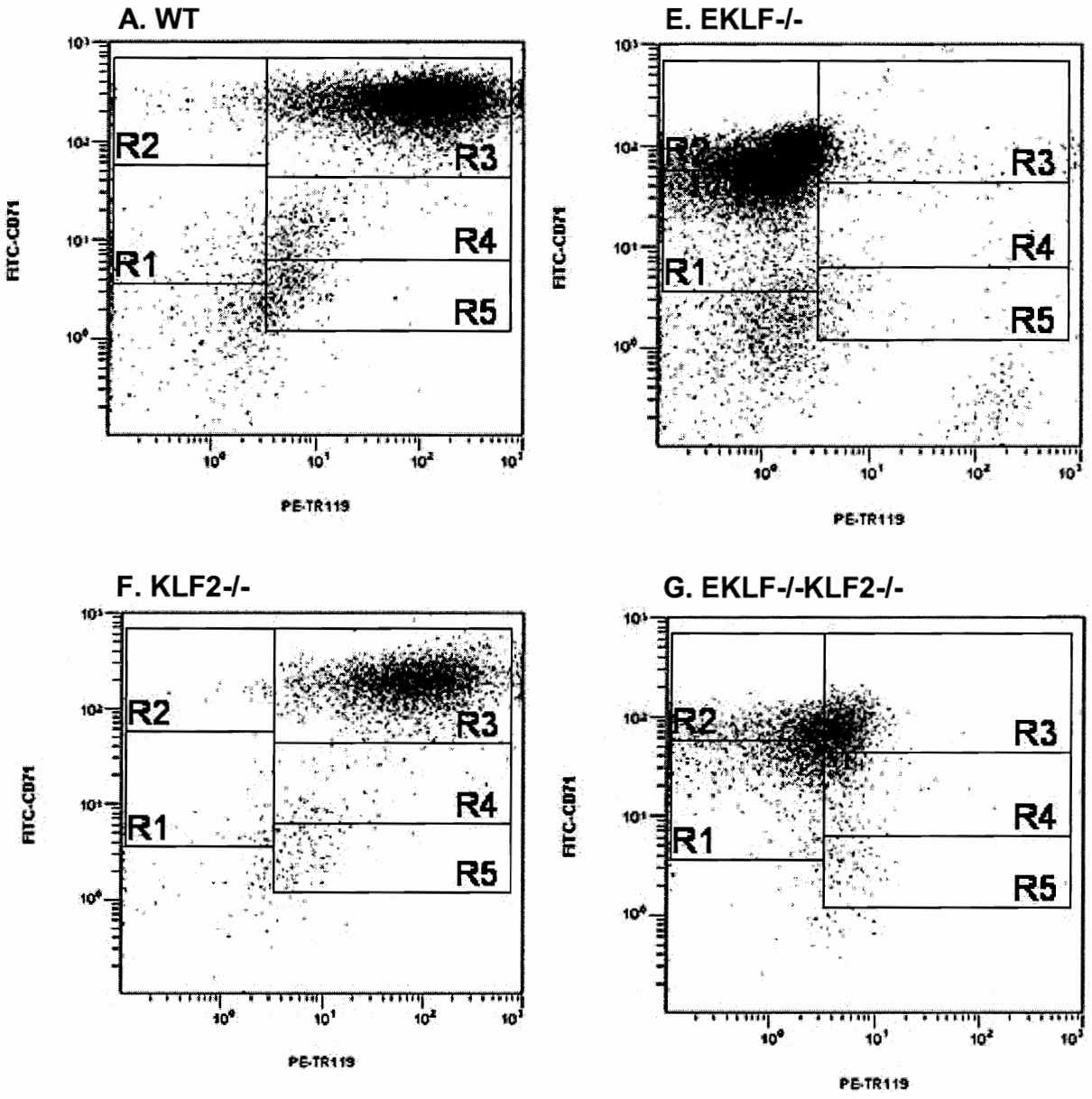

Figure 13A-G: Representative double-labeled FITC-CD71 and PE-TER119 histoplots from E9.5 blood. "A" gated populations were plotted to determine intensity of cells staining for both CD71 and TER119. (Refer to FSC/SSC plots for "A" region) A) WT. High levels of TER119 and CD71 staining. B) EKLF+/-. C) KLF2+/-. D) EKLF+/-KLF2+/-. E) EKLF-/-. F) KLF2-/-. G) EKLF-/-KLF2-/-. "R1-R5" gates are drawn according to Zhang et al (2003) and flow cytometry controls.

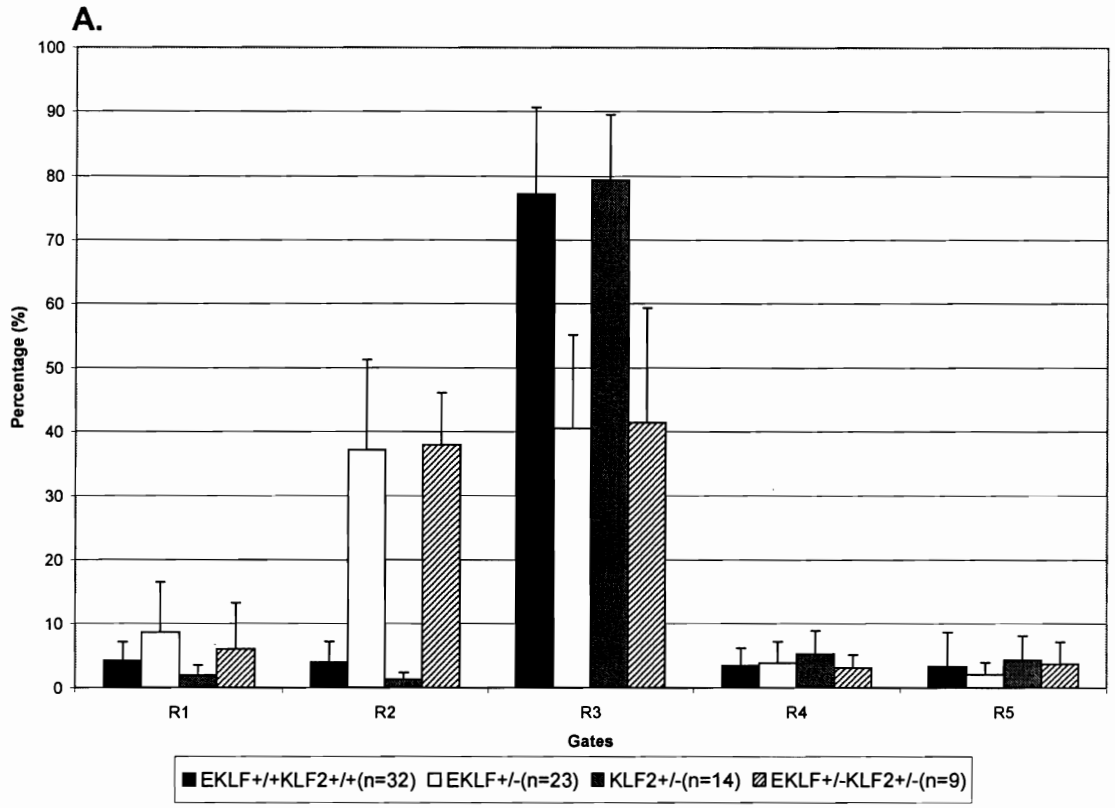
A.
100
90
80
70
60
50
40
30
20
10
0
Percentage (%)
R1
R2
R3
R4
R5
Gates
EKLF+/+KLF2+/+(n=32)
EKLF+/-(n=23)
KLF2+/-(n=14)
EKLF+/-KLF2+/-(n=9)

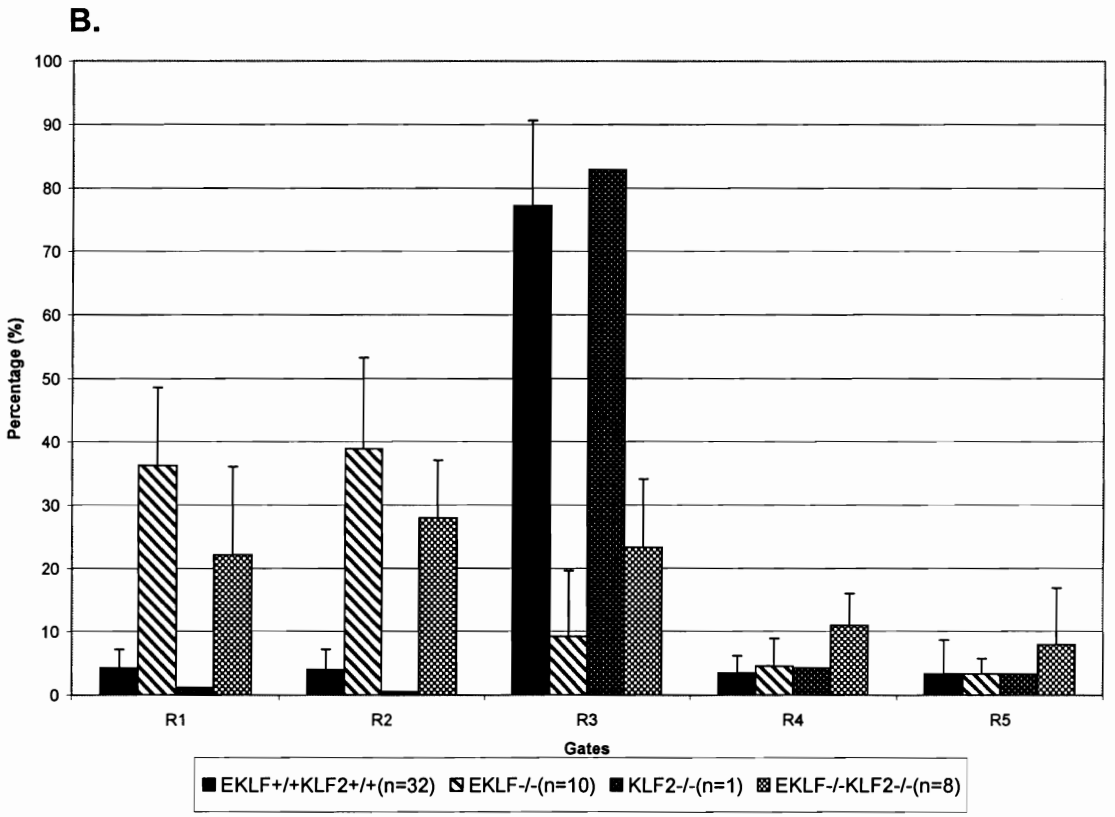
B.
100
90
80
70
60
50
40
30
20
10
0
Percentage (%)
R1
R2
R3
R4
R5
Gates
EKLF+/+KLF2+/+(n=32)
EKLF-/-(n=10)
KLF2-/-(n=1)
EKLF-/-KLF2-/-(n=8)

Figure 14A and B: Maturational Changes in E9.5 Erythroid Cells from EKLF+/- only, KLF2+/- only, and EKLF+/-KLF2+/- heterozygous matings. Primitive erythroid cells were double-labeled FITC-CD71 and PE-TER119 histoplots from E9.5 blood. "A" gated populations were plotted to determine intensity of cells staining for both CD71 and TER119. (Refer to FSC/SSC plots for "A" region). Depending on where cells fell in regions R1-R5 (See Figure 13), average percentages were calculated from each region and corrected to total average WT percentages. In Panel A, E9.5 blood from WT was compared to EKLF+/-, KLF2+/-, and EKLF+/-KLF2+/-. In Panel B, WT was compared to knockouts in EKLF, KLF2, and EKLF/KLF2. These results can be seen in the data table which follows.

Table 5: Data Table of Corrected Percentages of CD71 and TER119 Labeled Primitive Erythroid Cells Plotted in Regions R1-R5. ☐ marks the region and genotype which differed significantly from WT at p-value<0.025. ♦ signifies the region in EKLF-/-KLF2-/- that was significantly different from EKLF-/- and from WT. ± value signifies standard deviation.

	EKLF+/+ KLF2+/+	EKLF-/-	**KLF2-/-	EKLF-/-KLF2-/-
R1	4.3±2.9	36.3±12.3	1.2	22.1±14.0
R2	4.0±3.2	38.9±14.4	0.6	28.0±9.1
R3	77.2±13.4	9.2±10.4	83.0	♦23.3±10.8
R4	3.5±2.7	4.6±4.3	4.3	♦10.9±5.1
R5	3.4±0.9	3.3±2.4	3.3	8.0±8.9

**No statistical analysis was done with KLF2-/-, n=1.

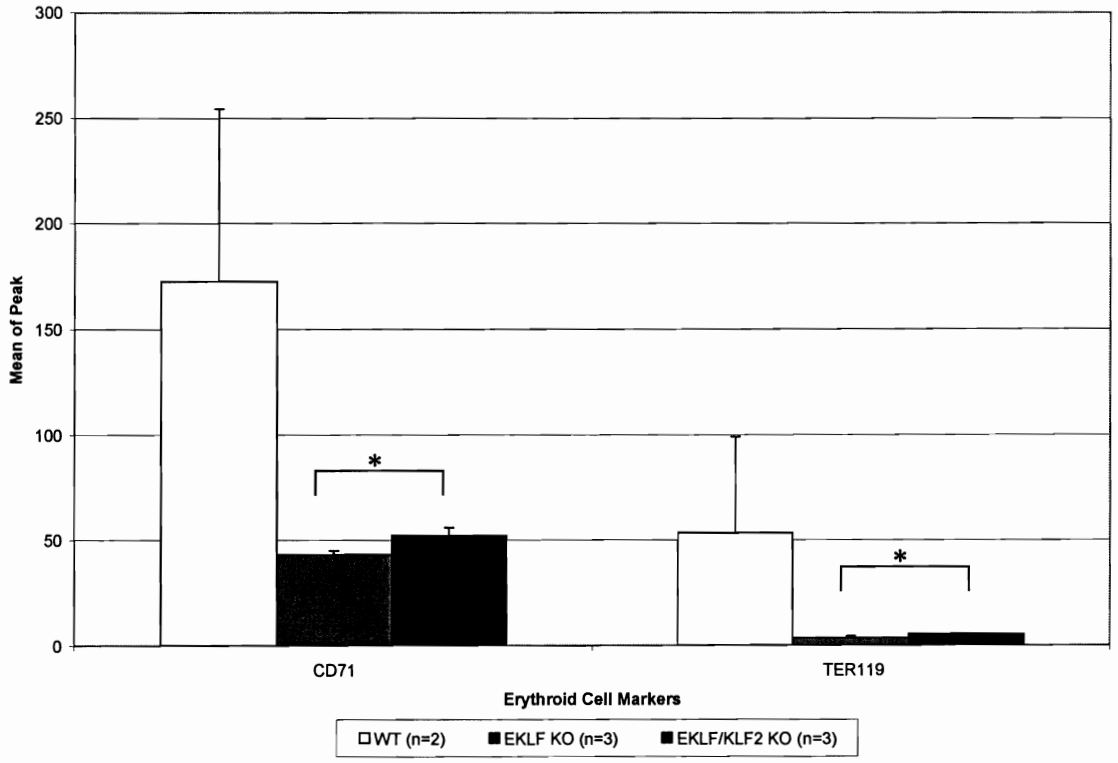

Figure 15: Mean Intensity of Sorted Primitive Erythroid Cells Labeled with CD71 and TER119 Antibodies. Error bars represent standard deviation. "*" represent significant to each other. Both EKLF-/- and EKLF-/-KLF2-/- are significantly different from WT.

CHAPTER 4

DISCUSSION

Earlier embryonic lethality of EKLF/KLF2 KO indicates more severe phenotype than single knockouts

EKLF/KLF2 KO embryos die by E11.5, which is earlier than the E12.5-E14.5 death of KLF2 KO and E14.5-E16.5 death of EKLF KO (Wani, 1998; Perkins, 1995). At E10.5 (Figure 4C-F), the double KO embryos appear anemic and developmentally stunted and have pale yolk sacs. E10.5 yolk sac embryonic globin mRNA also was significantly more decreased compared to WT in the double KO. Neither EKLF KO nor KLF2 KO show as dramatic a decrease in globin mRNA as seen in the double KO. Developmental deficits in the double KO embryo and yolk sac lead to early embryonic death at E11.5. The quantification of the number of abnormal erythroid, endothelial and mesothelial cells in E9.5 EKLF/KLF2 proved significantly higher than WT and KLF2 KO, likely leading to earlier embryonic death than the KLF2 KO.

Migration of EKLF/KLF2 KO primitive erythroid cells from yolk sac to embryo

By studying the E9.5 double KO yolk sac and also embryonic aorta, it was shown that primitive erythroid cells produced in the yolk sac can successfully migrate to the embryo. This indicates that in the EKLF/KLF2 KO embryos, not only has primitive erythropoiesis occurred, but also that the mouse circulation has fused between yolk sac

and embryo, as normally occurs at approximately E8.5. No obvious anemia could be reported in E9.5 EKLF/KLF2 KO embryos; however, a day later at E10.5, anemia was apparent in EKLF/KLF2 KO yolk sacs and embryos (Basu, unpublished). In E9.5 single KO, double KO, and WT embryos and yolk sacs, both normal and irregularly-shaped erythroid cells were present. As expected, the number of abnormal erythroid cells in the double KO yolk sac was significantly greater than either EKLF KO or KLF2 KO. Nevertheless, it is clear that primitive erythropoiesis has occurred to some extent, even in the double KO embryos.

Morphological changes in yolk sac are possible contributors to early death

Histologically, the E9.5 mouse yolk sac of EKLF/KLF2 KO showed unexpected developmental problems. The erythroid, endothelial and mesothelial cells appeared abnormal in the double KO yolk sac when compared to WT and KLF2 KO yolk sacs. Although not investigated in this study, EKLF KO yolk sacs were examined at E12.5 (Drissen, 2005).

In the analysis of erythroid cells of the EKLF KO yolk sac, previous studies show evidence of defective primitive erythropoiesis. At E12.5, EKLF KO yolk sac erythroid cells were abnormal with blue-staining inclusion or Heinz bodies, which appeared to be α-globin aggregates (Drissen, 2005). In this study, these bodies were not observed in E9.5 EKLF/KLF2 KO or KLF2 KO yolk sac erythroid cells. In E10.5 KLF2 KO yolk sac, there were about 2-fold more abnormal erythroid cells than WT and 5-fold more apoptotic cells (Basu, 2006). Interestingly, in E9.5 KLF2 KO, yolk sac did not contain a

significantly different percentage of abnormal erythroid cells compared to WT; this may indicate KLF2 becomes functionally active between E9.5 and E10.5. According to the criteria set forth in this study, E9.5 abnormal yolk sac erythroid cells were significantly increased (19-fold) in EKLF/KLF2 KO compared to both WT and KLF2 KO. No perceived anemia was present in the E9.5 double KO or KLF2 KO yolk sacs when compared to WT, in whole mount or histological sections. Eventually at E10.5, double KO yolk sacs were pale and embryos were anemic (Basu, under revision), which supports the assertion that KLF2 has functional importance after E9.5. The phenotype of EKLF/KLF2 KO yolk sac primitive erythroid cells suggests that globin expression is not the only abnormality.

In the E12.5 EKLF KO yolk sac, no abnormalities were reported in endothelial cells, although this was not a primary focus of the study (Drissen, 2005). While EKLF has not been implicated in the function of endothelial cells, KLF2 has been strongly implicated in vascular and endothelial cell development. According to Wani et al. (1998), KLF2 KO yolk sac vasculature appeared normal at E11.5, but pale by E12.5. E9.5 double KO yolk sacs showed a 32-fold increase in abnormal endothelial cells compared to WT, whereas the KLF2 KO was not significantly different from WT. Morphologically in the double KO, abnormal endothelial cells appeared non-squamous and inappropriately protruded into the yolk sac blood vessels. While endothelial cells are a confirmed target of KLF2, this work indicates for the first time that they are also affected by EKLF, as seen in the remarkable change in the double KO compared to single KOs. The double KO endothelial cells are affected at an early developmental time point, when the KLF2

KO endothelial cells are not. Additional evidence supports analogous regulation of endothelial and erythroid cells due to their closely related ontogeny based on both originating from the mesoderm germ layer (Minko, 2003). The theories of the ontogenic relationship between the two cells are based upon either a common precursor between endothelial and erythroid cells termed hemangioblast or that erythroid cells are derived from hemogenic endothelium (Choi, 1998; Li 2005).

Abnormal yolk sac mesothelial cells have not been documented in either EKLF KO or KLF2 KO. E9.5 double KO embryonic yolk sacs had a significantly (4-fold) higher percentage of abnormal mesothelial cells than did WT and KLF2 KO. These novel results support the hypothesis that development is dramatically more affected in EKLF/KLF2 KO than in KLF2 KO. It is not certain whether this means the mesothelial cell is a direct target of EKLF or KLF2, or if the cell is reacting to the absence of EKLF or KLF2 in other cell types. However, mesothelial cells also have a mesodermal origin.

Irregular yolk sac endothelial cells are located adjacent to mesothelial but not epithelial cells, indicating a spatial-effect in EKLF/KLF2 KO

In E9.5 EKLF/KLF2 KO yolk sac, there were 38-fold more abnormal endothelial cells on the mesothelial (60.7%) than on the endodermal epithelial cell side (1.6%). This introduces the possibility of a disturbance in the interaction between the erythroid, endothelial, and mesothelial cell layers. The mesothelial cell layer lacks the robust nature and structure of the endodermal epithelial cell layer which may explain why most of the abnormal endothelial cells in double KO were found on the mesothelial cell layer side. Both epithelial and mesothelial layers function as primary absorptive layers between

maternal and fetal tissues (Pendergrass, 1982). There is evidence suggesting that visceral and parietal endoderm of the yolk sac provides inductive signals aiding in the development of erythroid and endothelial cells (Miura, 1969; Belaousoff, 1999; Palis 1995; Yoder, 1994). Taken together, this shows that EKLF and KLF2 may largely target mesodermally derived tissues such as endothelial and mesothelial cells on the visceral yolk sac. Another explanation is that EKLF loss in erythroid cells can lead to defective developmental signals passed to the endothelial and mesothelial layers to change their morphology as well as negatively affect embryo development. This should be considered because EKLF is expressed only in erythroid cells. In addition, since EKLF mRNA was found in the primitive streak of the chicken, this could point to an earlier global role of EKLF in progenitors (Chervenak, 2006). However, mouse EKLF mRNA has not been noted in primitive streak, either because it is not there, or is transiently expressed and was not detectable.

Although there were many more normal than abnormal endothelial cells found adjacent to the epithelial cell layer in the double KO yolk sac, epithelial cells did demonstrate changed morphology in the form of invaginations. Due to the rarity of these, it may or may not be a significant finding in the double KO. Or, the epithelial invaginations may occur due to instability of other cell layers, not due to abnormalities in the epithelial cells themselves.

EKLF and KLF2 function in early embryos

In E9.5 embryos, the dorsal aortae were examined. Because the aortae are part of the transient definitive erythropoiesis site, the AGM (aorta-gonado-mesonephros), it may be a potential EKLF and KLF2 target. In situ analyses of E9 embryos showed that EKLF mRNA is expressed near the dorsal aortae (Southwood, 1996). Beginning at E9.5, KLF2 expression was found throughout the embryo vasculature by in situ hybridization (Kuo, 1997). E11.5 KLF2 KO embryos do not have any overt organ abnormalities, which is one to three days prior to KLF2 KO embryonic lethality (Wani, 1998). Kuo et al (1997) showed that at E12.5, abnormal, non-squamous, cuboidal endothelial cells surround KLF2 KO embryo dorsal aortae. The loss of KLF2 in endothelial cells, leads to embryonic heart failure and lethality by E14.5 (Lee, 2006).

In the E9.5 KLF2 KO examined in this study, dorsal aorta showed no defective endothelial or erythroid cells. However, in the E9.5 double KO dorsal aorta, erythroid and endothelial cells showed the same phenotype as those in the yolk sac. Erythroid cells also showed irregular shapes in the form of multiple cytoplasmic projections. This indicates that at E9.5, the double KO affects yolk sac and embryo endothelial cells, although the single KLF2 KO does not. Again, KLF2 may not be functionally active until after E9.5, though KLF2 mRNA has been confirmed at this stage. Also, the double KO phenotype may be caused by the loss of EKLF in erythroid cells subsequently triggering other endothelial-specific gene targets to lose function, which could be located in either erythroid or endothelial cells. As a control, E9.5 EKLF KO embryos should be examined next, though it is not expected that endothelial defects will be observed.

Cytospins confirm erythroid cell membrane abnormalities with loss of EKLF

In previous studies, it was suggested that EKLF is not necessarily required in developing progenitors, but is absolutely essential in terminal differentiation of definitive erythroid precursors (Nuez, 1995). Similarly, KLF2 regulation of embryonic globins in primitive erythroid cells suggested a role in the later stages of differentiation of erythroid cells (Basu, 2005). E12.5 EKLF KO nucleated primitive erythroid cells had abnormal membrane morphology in cytospins, characterized by wrinkles and deformity (Drissen, 2005). In the E12.5 EKLF KO definitive erythroid cells, several crucial membrane proteins are downregulated. In this study, E9.5 KLF2 KO primitive erythroid cells showed morphology similar to WT. From this, the question arose whether E9.5 EKLF KO contained morphologically normal primitive erythroid cells and, furthermore, whether the E9.5 double KO had the same characteristics.

The morphology of E9.5 double KO primitive erythroid cells was significantly altered when compared to WT and KLF2 KO. Although the morphology in double KO cells was more drastically altered than EKLF KO E9.5 erythroid cells, the percentage of abnormal cells was not statistically different. EKLF KO erythroid cells had multiple cytoplasmic protrusions resulting in misshapen, but yet still round cells. However, the double KO erythroid cells had elongation and larger portions of cytoplasm protruding out of the cell. In comparison, the EKLF KO E9.5 primitive cells looked similar to the EKLF KO E12.5 primitive cells (Drissen, 2005). This suggests that EKLF has an earlier role in primitive differentiation than previously recognized. Also, since the role of KLF2 in primitive erythroid cells had been documented by embryonic globin levels in the KLF2

KO at E10.5, the more severe double KO phenotype at E9.5 shows that KLF2 could target other primitive erythroid genes such as membrane proteins. Due to a similar DNA-binding motif, KLF2 and EKLF could share essential membrane protein gene targets. Gene expression of these EKLF targets should be examined in the KLF2 KO and double KO.

Maturational profiles of primitive erythroid cells show EKLF has a role in erythroid differentiation

Primitive erythropoiesis was the large focus of this study because of its direct correlation with embryo development; additionally, embryonic globin is a confirmed regulatory target of both EKLF and KLF2. Besides the morphological changes in cytospins, it was important to describe the maturational stage of erythroid cells at E9.5 by using flow cytometry. This would give a more in depth understanding of how EKLF and KLF2 affect the primitive erythroid cell. At E10.5, double KO yolk sacs had one-fifth of the normal amount of embryonic β-like globin mRNA (Basu, under revision for *Blood*) but normal amounts of the cell membrane protein glycophorin A (GPA) mRNA. In definitive erythroid cells, the amount of EKLF transcripts correlates to the amount of TER119 cell surface marker expression, such as seen in haploinsufficiency (Drissen, 2005). While normal E10.5 double KO (Basu, under revision) GPA levels indicated that erythroid cells developed at least through the proerythroblast stage or R2 (according to gates set by Zhang, et al. 2003), it seemed that they were stunted at some later stage as evidenced by the low globin mRNA compared to normal. This is similarly seen in the

adult erythroid cells in the EKLF KO, which are unable to terminally differentiate (Coghill, 2001).

The flow cytometry data suggests that E9.5 double KO erythroid cells do not differentiate normally, as evidenced by the significantly different distribution of cells among gates R1 - R5. In gates R1-R4, the percentage of double KO cells was significantly different from WT cells. Histoplots of cells labeled with FITC and PE with their mean peak intensity show that both TER119 and CD71 expression is significantly lowered in the double KO. This demonstrates that TER119 and transferrin receptor are not manufactured as in normal WT erythroid cells. Interestingly, cells labeled differently for KLF2 KO and EKLF KO. KLF2 KO cells have levels of TER119 expression similar to WT. A lowered TER119 marker intensity in EKLF KO and EKLF/KLF2 KO cells suggests that many cells do not become differentiated past a certain stage, most likely proerythroblast. Compared to EKLF KO, mean TER119 and CD71 marker intensity was significantly higher in the double KO, however by only 1.5-fold. Since the double KO has lower transferrin receptor levels than WT and KLF2 KO, this suggests that most double KO cells do not reach the basophilic erythroblast stage. Collectively, double KO cells could be developmentally stunted at the proerythroblast stage. E9.5 EKLF KO showed significantly reduced levels of CD71 expression, which is not seen in E11.5 EKLF KO (Drissen, 2005). KLF2 KO or KLF2+/- did not show any significant TER119 or CD71 differences from WT. Primitive erythroid cells appeared the same in KLF2+/- and KLF2 KO further supporting the assertion that KLF2 has no bearing on erythroid cell differentiation. However, KLF2 must have some enhanced effect in the absence of

EKLF because in the case of simultaneous ablation in double KO primitive erythroid cells, they have more severe morphology than EKLF KO. However, the flow cytometry analysis yields similar results for EKLF KO and EKLF/KLF2 KO, thereby showing a strong contribution of the ablation of EKLF to the abnormal phenotype of EKLF/KLF2 KO.

It was originally reported that ablation of KLF2 did not change EKLF mRNA expression in E11.5 embryos (Wani, 1998); but, it was later found that EKLF mRNA was decreased 2-fold in E10.5 KLF2 KO yolk sac (Basu, unpublished). In this study, E9.5 KLF2 KO primitive blood cells did not have any obvious morphological defects or maturational profile changes. However, EKLF KO erythroid cell TER119/CD71 histoplots do not appear identical to double KO erythroid cell TER119/CD71 histoplots. E9.5 EKLF KO and double KO maturational profiles were only significantly different (2.5-fold higher in double KO) in R3 and R4 gates, which were unexpected results. This suggests that E9.5 double KO erythroid cells are more mature than EKLF KO. Possible explanations are that double KO primitive erythroid cells are not more immature than EKLF KO cells. However, it is also plausible that this simple assay cannot explain the maturational problems in the double KO cells. The unexpected distribution could be attributed to severely altered cell membranes, which affected the ability of membrane proteins such as TER119 and transferrin receptor to be recognized in the assay. Overall, double KO primitive erythroid cells appear to have more defective cell morphology and increased membrane deformities compared to EKLF KO cells.

EKLF and KLF2 necessary for primitive erythroid differentiation

Both EKLF and KLF2 are implicated in embryonic globin gene regulation, but now both have been determined to be involved in primitive differentiation programs or stabilization of cells. Parallel changes in erythroid cell morphology occurred in EKLF KO primitive and definitive cells. E9.5 KLF2 KO primitive erythroid cells did not seem to be malformed, but the E9.5 EKLF/KLF2 KO demonstrated the early involvement of the KLFs in erythropoiesis. By E10.5, KLF2 KO primitive erythroid cells in yolk sac appeared abnormal, which indicates that erythropoiesis is KLF2-dependent (Basu, 2006). Comparing the KLF2 KO yolk sac at E9.5 to E10.5, results show that KLF2 may target erythroid temporal-specific genes. Similar DNA-binding motifs for EKLF and KLF2 suggest similar gene targets.

This may explain the more dramatic cell morphology of EKLF/KLF2 KO. EKLF and KLF2 have confirmed compensatory roles in globin regulation, but this work shows that they also likely have compensatory roles in the regulation of other genes, possibly membrane proteins. The two KLFs are unable to completely substitute for each other; otherwise single KO embryos would have normal erythroid cells. However, EKLF and KLF2 do have overlapping functions.

There are many questions that remain to be answered in the future. For example, it will be important to determine which genes in which cell types are regulated by both EKLF and KLF2. Clearly, cardiovascular development and erythropoiesis are intricately related, and more studies are required to test the roles of these two factors in developmental regulation. Additionally, if EKLF mRNA is present in chicken prior to

blood island formation, possibly in a stem cell, this may hold true for mouse as well. By extension, this may mean that KLF2 could be transiently active at this point to suggest that both EKLF and KLF2 are present in a common progenitor of erythroid and endothelial cells.

EKLF and KLF2 may have more relevance to hemoglobinopathies, due to similar erythroid cell phenotypes and globin expression found in knockout models. Sickle cell anemia involves a defective globin protein; this causes abnormal cell shapes perhaps due to erythroid membrane defects, as similarly seen in EKLF/KLF2 KO. Similarly, KLF2 KO can be used to study cardiovascular diseases. Therapies targeting primitive erythropoiesis can ultimately be designed to treat genetic diseases.

LIST OF REFERENCES

Literature Cited

Anderson, K., Kern, C., Crable, S., Lingrel, J. (1995) Isolation of a gene encoding a functional zinc finger protein homologous to erythroid kruppel-like factor: identification of a new multi gene family. Molecular and Cellular Biology *15*, 5957-5965.

Baron, M. (2003) Embryonic origins of mammalian hematopoiesis. Experimental Hematology *31*, 1160-1169.

Basu, P., Lemsaddek, W., Lung, T., Giang Sargent, T., Basu, M., Redmond, L., Lingrel, J., Haar, J., Lloyd, J. (under revision) EKLF and KLF2 have compensatory roles in embryonic β-globin gene expression and primitive erythropoiesis. Blood.

Basu, P., Morris, P.E., Haar, J., Wani, M., Lingrel, J., Gaensler, K., Lloyd, J. (2005) KLF2 is essential for primitive erythropoiesis and regulates the human and murine embryonic β-like globin genes in vivo. Blood *106*, 2566-2571.

Belaoussoff, M., Farrington, S., Baron, M. (1998) Hematopoietic induction and respecification of A-P identity by visceral endoderm signaling in the mouse embryo. Development *125*, 5009-5018.

Bieker, J., Southwood, C. (1995) The erythroid kruppel-like factor transactivation domain is a critical component for cell-specific inducibility of a β-globin promoter. Molecular and Cellular Biology *15*,852-860.

Bielinska, M., Narita, N., Heikinheimo, M., Porter, S., Wilson, D. (1996) Erythropoiesis and vasculogenesis in embryoid bodies lacking visceral yolk sac endoderm. Blood *88*, 3720-3730.

Brekelmans, P., van Soest, P., Voerman, J., Platenburg, P., Leenen, P., van Ewijk, W. (1994) Transferrin receptor expression as a marker of immature cycling thymocytes in the mouse. Cell Immunology *159,* 331-339.

Carlson, C., Endrizzi, B., Wu, J., Ding, X., Weinreich, M., Walsh, E., Wani, M., Lingrel, J., Hogquist, K., Jameson, S. (2006) Krüppel-like factor 2 regulates thymocyte and T-cell migration. Nature *442*, 229-302.

Chervenak, A., Basu, P., Shin, M., Redmond, L., Shen, G., Lloyd, J. (2006) Identification, characterization and expression pattern of the chicken EKLF gene. Developmental Dynamics *235*, 1933-1940.

Choi, K. (2002) The hemangioblast: a common progenitor of hematopoietic and endothelial cells. Journal of Hematotherapy and Stem Cell Research *11*, 91-101.

Coghill, E., Eccleston, S., Fox, V., Cerruti, L., Brown, c., Cunningham, J., Jane, S., Perkins, A. (2001) Erythroid Kruppel-like factor (EKLF) coordinates erythroid cell proliferation and hemoglobinization in cell lines derived from EKLF null mice. Blood *97*, 1861-1868.

Cumano, A., Godin, I. (2001) Pluripotent hematopoietic stem cell development during embryogenesis. Current Opinion in Immunology *13*, 166-171.

Cumano, A., Dieterlien-Lievre, F., Godin, I. (2000) The splanchnopleura/AGM region is the prime site for the generation of multipotent hemopoietic precursors, in the mouse embryo. Vaccine *18*, 1621-1623.

Dekker, R., Boon, R., Rondaij, M., Kragt, A., Volger, O. Elderkamp, Y., Meijers, J., Voorberg, J., Pannekoek, H., Horrevoets, A. (2006) KLF2 provokes a gene expression pattern that establishes functional quiescent differentiation of the endothelium. Blood *107*, 4354-4363.

Drissen, R., von Lindern, M., Kolbus, A., Driegen, S., Steinlein, P., Beug, H., Grosveld, F., Philipsen, S. (2005) The erythroid phenotype of EKLF-null mice: defects in hemoglobin metabolism and membrane stability. Molecular and Cellular Biology *25*, 5205-5214.

Dumont D.J., Gradwohl, G., Fong, G.H., Puri, M.C., Gertsenstein, M., Auerbach, A. and Breitman, M.L. (1994) Dominant-negative and targeted null mutations in the endothelial receptor tyrosine kinase, tek, reveal a critical role in vasculogenesis of the embryo. Genes Dev., *8*, 1897–1909.

Durand, C., Dzierzak, E. (2005) Embryonic beginnings of adult hematopoietic stem cells. Hematology Journal *90*, 100-108.

Feng, W., Southwood, C., Bieker, J. (1994) Analyses of β-thalassemia mutant DNA interactions with erythroid Krüppel-like factor (EKLF), an erythroid cell-specific transcription factor. Journal of Biological Chemistry *269*, 1493-1500.

Fraser, S., Isern, J., Baron, M. (2007) Maturation and enucleation of primitive erythroblasts during mouse embryogenesis is accompanied by changes in cell-surface antigen expression. Blood *109*,343-351.

Fraser, S., Ogawa, M., Yokomizo, T., Ito, Y., Nishikawa, S., Nishikawa S. (2003) Putative intermediate precursor between hematogenic endothelial cells and blood cells in the developing embryo. Development, Growth and Differentiation *45*, 63-75.

Frenette, P., Atweh, G. (2007) Sickle cell disease: old discoveries, new concepts, and future promise. The Journal of Clinical Investigation *117*, 850-858.

Garcia-Porrero, J., Manaia, A., Jimeno, J., Lasky, L., Dieterlen-Lievre, F., Godin, I. (1998) Antigenic profiles of endothelial and hemopoietic lineages in murine intraembryonic hemogenic sites. Developmental and Comparative Immunology *22*, 303-319.

Gerety SS, Anderson DJ.(2003) Cardiovascular ephrin B2 function is essential for embryonic angiogenesis. Development. *129*, 1397–1410.

Haar, J.L. and Ackerman, G.A. (1971). A phase and electron microscopic study of vasculogenesis and erythropoiesis in the yolk sac of the mouse. The Anatomical Record *170*, 199-223

Hodge, D., Coghill, E., Keys, J., Maguire, T., Hartmann, B., McDowall, A., Mitchell, W., Grimmond, S., Perkins, A. (2006) A global role for EFKL in definitive and primitive erythropoeisis. Blood *107*, 3359-3370.

Hristoskova, S., Holzgreve, W., Hahn, S. (2003) Fetal nucleated erythrocytes in maternal circulation do not display a classic membrane-associated apoptotic characteristic (phosphatidylserine exposure) despite being positive by terminal dUTP nuclear end labeling. Clinical Chemistry *49*, 1934-1937.

Hu, X., Bulger, M., Roach, J., Eszterhas, S., Olivier, E., Bouhassira, E., Groudine, M., Fiering, S. (2003) Promoters of the murine embryonic β-like globin genes EY and βh1 do not compete for interaction with the β-globin locus control region. PNAS *100*, 1111-1115.

Jaffredo, T., Nottinham, W., Liddiard, K., Bollerot, K, Pouget, C., deBruijn, M. (2005) From hemangioblast to hematopoietic stem cell: an endothelial connection? Experimental Hematology *33,* 1029-1040.

Ji, R., Phoon, C., Aristizabal, O., McGrath, K., Palis, J., Turnball, D. (2003) Onset of cardiac function during early mouse embryogenesis coincides with entry of primitive erythroblasts into the embryo proper. Circulation Research *92*, 133-135.

Kingsley, P., Malik, J., Emerson, R., Bushnell, T., McGrath, K., Bloedorn, L., Bulger, M., Palis, J. (2006) "Maturational" globin switching in primary primitive erythroid cells. Blood *104*, 1665-1672.

Kingsley, P.D., Malik, J., Fantauzzo, K.A., and Palis, J. (2003). Yolk sac derived primitive erythroblasts enucleate during mammalian embryogenesis. Blood *104*, 19-25.

Koury, M., Sawyer, S., Brandt, S. (2002) New insights into erythropoiesis. Current Opinion in Hematology *9*, 93-100.

Kuo, C., Veselits, M., Barton, K., Lu M., Clendenin, C., Leiden, J. (1997) The LKLF transcription factor is required for normal tunica media formation and blood vessel stabilization during murine embryogenesis. Genes and Development *11*, 2996-3006.

Lee, J., Yu, Q., Shin, J., Sebzda, E., Bertozzi, C., Chen, M., Mericko, P., Stadtfeld, M., Zhou, D., Cheng, L., Graf, T., MacRae, C., Lepore, J., Lo, C., Kahn, M. (2006) KLF2 is an essential regulator of vascular hemodynamic forces in vivo. Developmental Cell *11*, 845-857.

Li, Q., Peterson, K., Fang, X., Stamatoyannopoulos, G. (2002) Locus control regions. Blood *100*. 3077-3086.

Li, W., Ferkowicz, M., Johnson, S., Shelley, W., Yoder, M. (2005) Endothelial cells in the early murine yolk sac give rise to CD41-expressing hematopoietic cells. Stem Cells and Development *14*, 44-54.

Lim, S., Bieker, J., Lin, C., Constantini, F. (1997) A shortened life span of EKLF-/- adult erythrocytes, due to a deficiency of β-globin chains, is ameliorated by human γ-globin chains. Blood *90*, 1291-1299.

Luo, H., Liang, X., Frye, C., Wonio, M., Hankins, G., Chui, D., Alter, B. (1999) Embryonic hemoglobins are expressed in definitive cells. Blood *94*, 359-361.

McGrath, K., Koniski, A., Malik, J., Palis, J. (2003) Circulation is established in a stepwise pattern in the mammalian embryo. Blood *101*, 1669-1676.

McGrath, K., Palis, J. (2005) Hematopoiesis in the yolk sac: more than meets the eye. Experimental Hematology *33*, 1021-1028.

Miller, I., Bieker, J. (1993) A novel, erythroid cell-specific murine transcription factor that binds to the CACCC element and is related to the Krüppel familiy of nuclear proteins. Molecular Cell Biology *13*, 2276-2786.

Minko, K., Bollerot, K., Drevon, C., Hallais, M., Jaffredo, T. (2003) From mesoderm to blood islands: patterns of key molecules during yolk sac erythropoiesis. Gene Expression Patterns *3*, 261-272.

Miura, Y., Wilt, F. (1969) Tissue interaction and the formation of the first erythroblasts of the chick embryo. Developmental Biology *19*, 201-211.

Morioka, K., Tone, S. Mukaida, M., Takano, H. (1998) The apoptotic and nonapoptotic nature of the terminal differentiation of erythroid cells. Experimental Cell Research *240*, 206-217.

Ney, P. (2006) Gene expression during terminal erythroid differentiation. (2006) Current Opinion in Hematology *13*, 203-208.

Nilson, D., Sabatino, D., Bodine, D., Gallagher. (2006) Major erythrocyte membrane protein genes in EKLF-deficient mice. Experimental Hematology *34*, 705-712.

Nuez, B., Michalovich, D., Bygrave, A., Ploemacher, R., Grosveld, F. (1995) Defective haematopoiesis in fetal liver resulting from inactivation of the EKLF gene. Nature *375*, 316-318.

Orkin, S.H. and Zon, L.I. (1997). Genetics of Erythropoisesis: Induced mutations in mice and zebrafish. Annual Review of Genetics *31*, 33-60.

Palis, J. (2004) No red cell is an island. Nature *432*, 964-965.

Palis, J. and Yoder, M.C. (2001). Yolk-sac hematopoiesis: The first blood islands of mouse and men. Experimental Hematology *29*, 927-936

Palis, J., Robertson, S., Kennedy, M., Wall, C., and Gordon, K. (1999). Development of erythroid and myeloid progenitors in the yolk sac and embryo proper of the mouse. Development *126*, 5073-5084.

Palis, J., McGrath, K., Kingsley, P. (1995) Initiation of hematopoiesis and vasculogenesis in murine yolk sac explants. Blood *86*, 156-163.

Pendergrass, P., Ream, L, Scott, J. (1982) Absorptive structures of the mouse yolk sac placenta and associated placental surfaces. A scanning electron microscope study. Journal of Submicroscopy Cytology *14*, 279-289.

Perkins, A., Sharpe, A., Orkin, S. (1995) Lethal β-thalassaemia in mice lacking the erythroid CACCC-transcription factor EKLF. Nature *375*, 318-322.

Porcu, S., Poddie, D., Melis, M., Cao, A., Ristaldi, M. (2005) β-minor globin gene expression is preferentially reduced in EKLF knock-out mice. Gene *351*, 11-17.

Ragoczy, T., Bender, M, Telling, A., Byron, R., Groudine, M. (2006) Genes and Development *20*, 1447-1457.

Robb, L. (1997) Hematopoiesis: Origin pinned down at last? Current Biology *7*, R10-R12.

Samokhvalov, I., Samokhvalova, N., Nishikawa, S. (2007) Cell tracing shows the contribution of the yolk sac to adult haematopoiesis. Nature *446*, 1056-1061.

Sasaki, K., Kendall, M. (1985) The morphology of the haematopoietic cells of the yolk sac in mice with particular reference to nucleolar changes. Journal of Anatomy *140*, 279-295.

Shalaby, F., Rossant, J., Yamaguchi, T., Gertenstein, M., Wu, X., Breitman, M., Schuh, A. (1995) Failure of blood-island formation and vasculogenesis in Flk-1-deficient mice. Nature *376*, 62-66.

Shyu, Y., Lee, T, Wen, S., Chen, H., Hsiao, W., Chen, X., Hwang, J., Shen C. (2007) Subcellular transport of EKLF and switch-on of murine adult β-major globin gene transcription. Molecular and Cellular Biology *27*, 2309-2323.

Socolovsky, M., Nam, H., Fleming, M., Haase, V., Brugnara, C., Lodish, H. (2001) Ineffective erythropoeisis in Stat5a-/-5b-/- mice due to decreased survival of early erythroblasts. Blood *98*, 3261-3273.

Southwood, C., Downs, K., Bieker, J. (1996) Erythroid Kriippel-like factor exhibits an early and sequentially localized pattern of expression during mammalian erythroid ontogeny. Developmental Dynamics *206*, 248-259.

Spadaccini, A., Tilbrook, P., Sarna, M., Crossley, M., Bieker, J., Klinken, P. (1998) Transcription factor erythroid Krüppel-like Factor (EKLF) is essential for the erythropoietin-induced hemoglobin production but not for proliferation, viability or morphological maturation. Journal of Biological Chemistry *273*, 23793-23798.

Stamatoyannopoulos, G. (2005) Control of globin gene expression during development and erythroid differentiation. Experimental Hematology *33*, 259-271.

Suzuki, T., Aizawa, K., Matsumura, T., Nagai, R. (2005) Vascular implications of the Krüppel-like family of transcription factors. Arteriosclerosis, Thrombosis, and Vascular Biology *25*, 1135-1141.

Terskikh, A., Miyamoto, T., Chang, C., Diatchenko, L., Weissman, I. (2003) Gene expression analysis of purified hematopoietic stem cells and committed progenitors. Blood *102*, 94-101.

Wakimoto, K., Kuro-o, M., Yanaka, N., Komuro, I., Nabeshima, Y., Imai, Y. (2001) Expression of Na /Ca2 exchanger (NCX1) gene in the developmental mouse embryo and adult mouse brain. Comparative Biochemistry and Physiology *130*, 191-198.

Wang, N., Miao, H., Li, Y., Zhang, P., Haga, J., Hu, Y, Young, A., Yuan, S., Nguyen, P., Wu, C., Chien, S. (2006) Shear stress regulation of Krüppel-like factor 2 expression is flow pattern-specific. Biochemical and Biophysical Research Communications *341*, 1244-1251.

Wani, M., Means, R., Lingrel, J. (1998) Loss of LKLF function results in embryonic lethality in mice. Transgenic Research *7*, 229-238.

Weiss, M., Orkin, S. (1995) Transcription factor GATA-1 permits survival and maturation of erythroid precursors by preventing apoptosis. PNAS *92*, 9623-9627.

Welch, J., Watts, J., Vakoc, C.,Yao, Y., Wang, H., Hardison, R., Blobel, G., Chodosh, L., Weiss, M. (2004) Global regulation of erythroid gene expression by transcription factor GATA-1. Blood *104*, 3136-3147.

Wong, P., Chung, S., Chui, D., Eaves, C. (1986) Properties of the earliest clonogenic hemopoietic precursors to appear in the developing murine yolk sac. PNAS *83*, 3851-3854.

Yoder, M., Papioannou, V., Breitfeld, P., Williams, D. (1994) Murine yolk sac endoderm-and mesoderm-derived cell lines support in vitro growth and differentiation of hematopoietic cells. Blood *83*, 2436-2443.

Zhang, J., Socolovsky, M., Gross, A., Lodish, H. (2003) Role of Ras signaling in erythroid differentiation of mouse fetal liver functional analysis by a flow cytometry-based novel culture system. Blood *102*, 3938-3946.

Zhou, D., Pawlik, K., Ren, J., Sun, C., Townes, T. (2006) Differential binding of erythroid Krüppel-like factor to embryonic/fetal globin gene promoters during development. Journal of Biological Chemistry *281*, 16052-16057.

Zon, L. (1995) Developmental Biology of Hematopoiesis. Blood *86*, 2876-2891.

APPENDIX

Appendix

Solutions

Millonig's Buffer

Solution A

Distilled H20	1000 ml
Sodium phosphate monobasic	22.6 g

Solution B

Distilled H20	250 ml
Sodium hydroxide	6.4 g

After dissolving, pour off 170 ml of Solution A and replace with 170 ml of Solution B.

VITA

Tina Kathy Lung was born on January 24, 1983 in Boston, Massachusetts, and is an American citizen. She graduated from Western Albemarle High School, Crozet, Virginia, in 2001. She received her Bachelor of Arts in Biology from University of Virginia, Charlottesville, Virginia in 2005.